A Description of the IVI-RA Model v0.1

Devin Incerti[*]   Jeroen P. Jansen[†]

July 11, 2017

Contents

---

[*]Innovation and Value Initiative
[†]Innovation and Value Initiative

List of Figures

List of Tables

1 Overview

This document describes version 0.1 of IVI's rheumatoid arthritis (RA) cost-effectiveness model. The IVI-RA model is an individual patient simulation (IPS) that simulates patients one at a time. The model reflects a range of perspectives (e.g., health care sector, societal) and structural assumptions. All told, there are 336 different model structures, which allows analysts to account for structural uncertainty. Parameter uncertainty is quantified with probabilistic sensitivity analysis (PSA).

The model is available as an R package with documentation available online. The source code can be viewed or downloaded at our GitHub repository. The IPS was primarily written in C++ so that PSA and analyses of structural uncertainty can be run in a reasonable amount of time. The model can either be run using R (see documentation) or online with our user-friendly R Shiny web application.

This document is structured as follows. We begin by discussing treatment strategies that can be modeled in Section 2. Section 3 outlines the competing model structures. Section 5 describes the statistical techniques used to estimate the model parameters and the data sources used. Section 4 examines the data needed to define a population and run an analysis. Finally, Section 6 describes the simulation techniques used to implement the RA family of models and quantify uncertainty.

2   Treatment strategies

The primary purpose of the model is to evaluate the cost-effectiveness of treatments for RA. Since patients typically use multiple treatments over a lifetime, the model is capable of simulating a treatment sequence of any arbitrary length. Treatments that can be included in a sequence include conventional disease-modifying anti-rheumatic drugs (cDMARDs) such as methotrexate as well as the following biologic DMARDS (bDMARDs):

- **Tumor necrosis factor (TNF) inhibitors**: etanercept, adalimumab, infliximab, certolizumab, golimumab

- **non-TNF inhibitors**: abatecept, tocilizumab, rituximab

- **Janus kinase/signal transducers and activators of transcription (JAK/STAT) inhibitors**: tofacitinib

At the end of a sequence, patient switch to non-biologic therapy (NBT), which encompasses a range of therapies that do not affect the rate of disease progression and are not associated with adverse events.

3   Competing model structures

The IVI-RA model is a discrete-time IPS with 6 month cycles that can be run using a number of different model structures. Like most RA cost-effectiveness models, the model measures changes in disease severity using the Health Assessment Questionnaire (HAQ) Disability Index score (Tosh et al. 2011; Carlson et al. 2015; Stephens et al. 2015; Stevenson et al. 2016; Institute for Clinical and Economic Review 2017; Stevenson et al. 2017). In particular, at the start of the simulation, each patient is assigned a baseline HAQ score. Subsequently, the impact of the disease measured by the HAQ trajectory over time is modeled as a function of a sequence of treatments (Figure 1). In the absence of treatment, HAQ deteriorates at a certain rate as depicted by the dashed line in the figure. Treatment is separated into two distinct phases: an initial phase of up to 6 months, consistent with data reported from randomized controlled trials (RCTs), and a maintenance phase thereafter until discontinuation.

During the initial treatment phase HAQ is modeled as a change from baseline. Three possible model structures labeled **H1-H3** are possible. In **H1**, treatment influences HAQ through its effect on the American College of Rheumatology (ACR) response criteria, which is similar to the structure used in other US based cost-effectiveness models (e.g. Carlson et al. 2015; Institute for Clinical and Economic Review 2017). ACR response is measured using four mutually exclusive categories: no response (defined as less than 20% improvement), ACR 20-50% improvement, ACR 50-70% improvement, and ACR 70% improvement or greater. The rationale for using ACR response rather than HAQ directly is that the evidence base relating treatment to ACR response is larger than the evidence based relating treatment to HAQ. **H2** follows the National Institute for Health and Care Excellence (NICE) cost-effectiveness model (Stevenson et al. 2016, 2017) and models the effect of treatment on HAQ indirectly through its effect on ACR response and, in turn, the three categories of the European League Against Rheumatism (EULAR) response (no response, moderate response, or good response). Finally, since modeling the effect of treatment on HAQ through intermediary variables may mediate treatment response, in **H3**, treatment impacts HAQ directly. The three scenarios are summarized below:
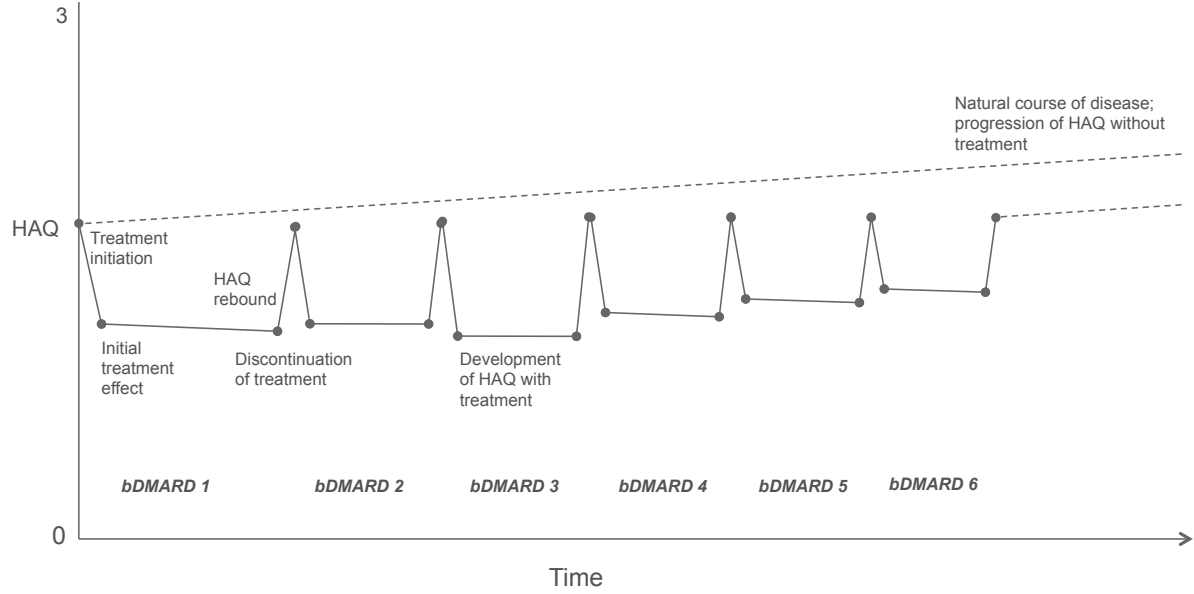
Figure 1: Model structure regarding development of HAQ with sequential biologic treatment

- **H1**: Treatment $\rightarrow$ ACR $\rightarrow$ HAQ

- **H2**: Treatment $\rightarrow$ ACR $\rightarrow$ EULAR $\rightarrow$ HAQ

- **H3**: Treatment $\rightarrow$ HAQ

The probability of switching treatment during the initial treatment phase is modeled using 6 possible structures labeled **S1-S6**. **S1** follows a common approach where ACR non-responders discontinue treatment (e.g. Carlson et al. 2015; Institute for Clinical and Economic Review 2017). One drawback of this approach is that it is not consistent with current treat-to-target guidelines in the United States (Singh et al. 2016). **S2** and **S3** consequently model treatment switching as a function of disease activity (remission, low, moderate, high) (Anderson et al. 2012). ACR response predicts the change in disease activity from baseline, which, along with baseline disease activity, predicts absolute disease activity. The probability of switching treatment is increasing in the severity of disease (i.e., the probability is lowest in remission and greatest with high disease activity). **S2-S4** measure disease activity using the Disease Activity Score with 28-joint counts (DAS28) (Prevoo et al. 1995), Simplified Disease Activity Index (SDAI) (Smolen et al. 2003; Aletaha and Smolen 2005), and Clinical Disease Activity Index (CDAI) (Aletaha et al. 2005) respectively.

S5 is similar to **S2-S4**, but models the effect of treatment on changes in DAS28 directly, rather than indirectly through ACR response. We also aimed to model the direct effect of treatment on SDAI and CDAI, but sufficient clinical trial data is not available. Finally, since in the UK, the British Society for Rheumatology and the British Health Professionals in Rheumatology recommends using the EULAR response (Deighton et al. 2010), treatment switching in **S6** depends on EULAR response. In particular, following the NICE model, we assume that EULAR non-responders discontinue treatment while moderate and good responders continue treatment (Stevenson et al. 2016). The reasoning is that rules stipulated by NICE require a DAS28 improvement of more than 1.2 to continue treatment which is associated with moderate or good EULAR response. The 6 treatment switching scenarios are summarized below:

- **S1:** Treatment → ACR → Switch

- **S2:** Treatment → ACR → ΔDAS28 → DAS28 → Switch

- **S3:** Treatment → ACR → ΔSDAI → SDAI → Switch

- **S4:** Treatment → ACR → ΔCDAI → CDAI → Switch

- **S5:** Treatment → ΔDAS28 → DAS28 → Switch

- **S6:** Treatment → ACR → EULAR → Switch

Not all model structures **S1-S6** can be used with each of **H1-H3**. If **H1** is used, then **S1-S5** are available, but **S6** is not because EULAR response is not simulated. In **H2**, **S1-S6** are all available while in **H3** only **S5** can be used since ACR response is not simulated. The 12 possible model structures and the number of each structure are outlined in Table 1.

Table 1: Model structures for initial treatment phase

	S1	S2	S3	S4	S5	S6
H1	1	2	3	4	5	-
H2	6	7	8	9	10	11
H3	-	-	-	-	12	-

Notes: Rows denote the model structure used to relate treatment to HAQ and columns denote the model structure used to predict treatment switching. Each number denotes a unique model structure (i.e. 1 corresponds to H1 and S1 and 8 corresponds to H2 and S3) and the "-" denotes a model structure combination that is not possible. There are 12 possible model structures for the initial treatment phase.

In the maintenance phase, two model structures can be used to simulate the long-term progression of HAQ. First, as is common in cost-effectiveness analyses (CEAs) of therapies for RA, HAQ is assumed to progress at a constant linear rate over time (see Tosh et al. 2011; Wailoo et al. 2008). However, since emerging evidence suggests that the rate of HAQ progression is non-linear (Gibson et al. 2015), our second scenario simulates HAQ progression using a latent class growth model (LCGM) (Norton et al. 2014) with 4 distinct HAQ trajectories and a rate of HAQ progression that decreases over time within each trajectory. Upon discontinuation of treatment, the HAQ score rebounds by a proportion of the improvement experienced at the end of the initial 6-month period with that treatment.

The duration of the maintenance phase (i.e., time to discontinuation of maintenance treatment) is simulated using parametric time-to-event distributions. When structure **S6** is used, the time-to-event distributions are stratified by EULAR response category. Patients with good response at the end of the initial treatment phase stay on treatment longer, on average, than patients with a moderate response. In contrast, when **S1** is used, time to treatment discontinuation is simulated using a single time-to-event curve because we have been unable to obtain curves stratified by ACR response categories. Likewise, when **S2-S5** are selected, we use a single time-to-event curve because we have not obtained curves stratified by disease activity level. In each case, time to discontinuation can be simulated using one of 7 possible distributions (exponential, Weibull, Gompertz, normal, gamma, log-logistic, generalized gamma).

In line with Stevenson et al. (2016) the adverse events included in the model are limited to serious infections; we assume that only serious infections have a significant cost impact and increased risk

over background rates to be meaningful to include (Ramiro et al. 2017). While on a treatment, a patient experiences a serious infection if the individual's sampled time to the adverse event is shorter than the sampled time to treatment discontinuation.

Baseline HAQ scores (and changes in HAQ scores from baseline) are used to determine mortality relative to age/sex specific rates for the US general population (assumed to have a HAQ score of 0). Treatment therefore has an indirect effect on mortality through its effect on HAQ.

Individual HAQ scores at a particular point in time were also used to simulate EQ-5D utility scores (0-1 range), which, in turn, were used to simulate quality-adjusted life-years (QALYs). However, since a number of different methods have been used to convert HAQ into utility, our model contains two different possible mapping algorithms. Our preferred algorithm is the Alava et al. (2013) mixture model, which uses a much larger sample size than other statistical models and has been shown to have better predictive accuracy. Other algorithms are typically estimated using clinical trial data (e.g. Carlson et al. 2015; Stephens et al. 2015) and consequently have limited generalizability. The second utility algorithm available within our model is based on a linear regression analysis of real-world data by Wailoo et al. (2006) that has been used in a few previous CEAs (e.g. Wailoo et al. 2008; Institute for Clinical and Economic Review 2017).

Annual hospitalization days and productivity losses are simulated as a function of HAQ. Health sector costs considered in the models are related to drug acquisition and administration, adverse events, general management of RA, and hospitalization. Non-health sector costs considered are limited to work related productivity loss.

Patient preferences for treatment attributes have a direct effect on long-term treatment duration and utility. Patients with treatments that more closely match their preferences have longer treatment duration and higher utility. Treatment attributes that are incorporated into the models include route of administration and frequency of administration.

The flow diagram in Figure 2 describes the flow of a single patient through the simulation. Each patient begins the simulation by initiating treatment and ends the simulation with death. The rectangles in the figure represent "processes" determining the effect of treatment on disease progression and the diamonds represent "decisions" that determine whether a patient will switch to a new treatment.

The influence diagram in Figure 3 summarizes the assumed structural relationships among different variables in the model. Each arrow represents the direct effect of one parameter on another. Dashed lines represent relationships that depend on the structural assumptions used. Figure 3a focuses on the effect of treatment on disease progression and adverse events while Figure 3b looks at the variables influencing the primary health and cost outcomes.

Model outcomes depend on patient characteristics, which have a direct effect on HAQ progression, mortality, and utility. The primary health outcome is the quality-adjusted life-year (QALY), which depends on mortality and utility. Total costs consist of health care sector costs and productivity losses. The components of health sector costs include drug acquisition and administration costs, general management and monitoring costs, adverse event costs, and hospitalization costs Analyses from a societal perspective would include productivity losses while analyses from a health care sector perspective would not. The value of treatment is estimated using the net-monetary benefit (NMB), which is calculated by multiplying QALYs by a willingness to pay threshold and subtracting costs ($NMB = QALYs \cdot WTP - Costs$).

Table 2 summarizes the competing model structures, which are conditional on the perspective of the decision maker. In total, there are 12 x 2 x 7 x 2 = 336 possible model structures.
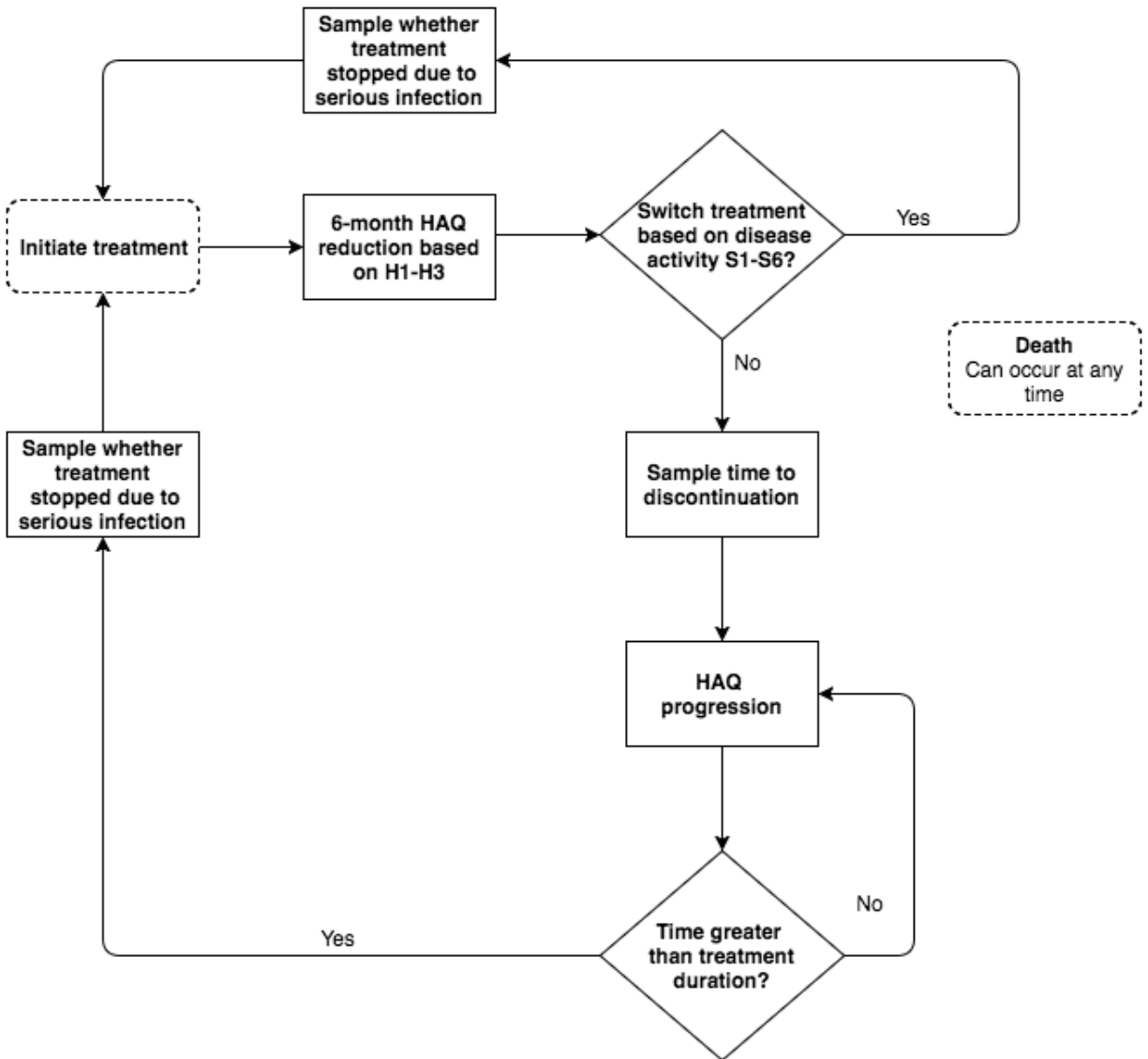
Figure 2: Flow diagram of the simulation for a single patient
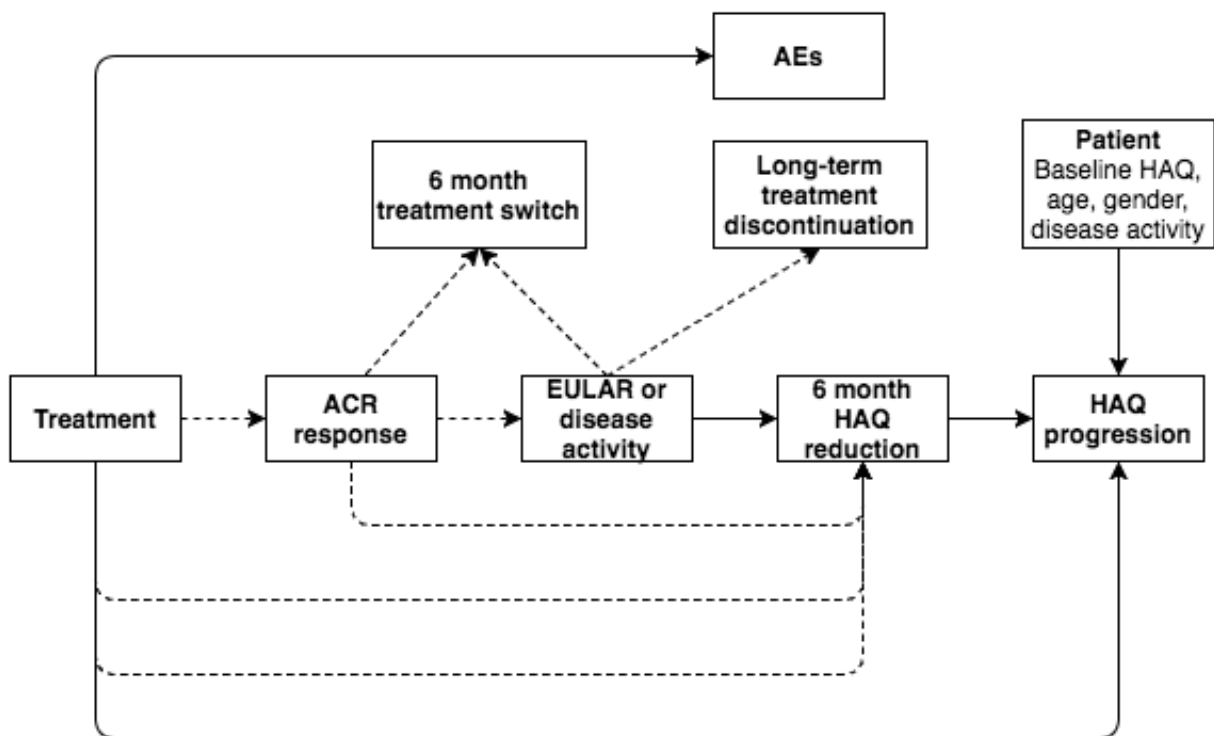
(a) Treatment effects
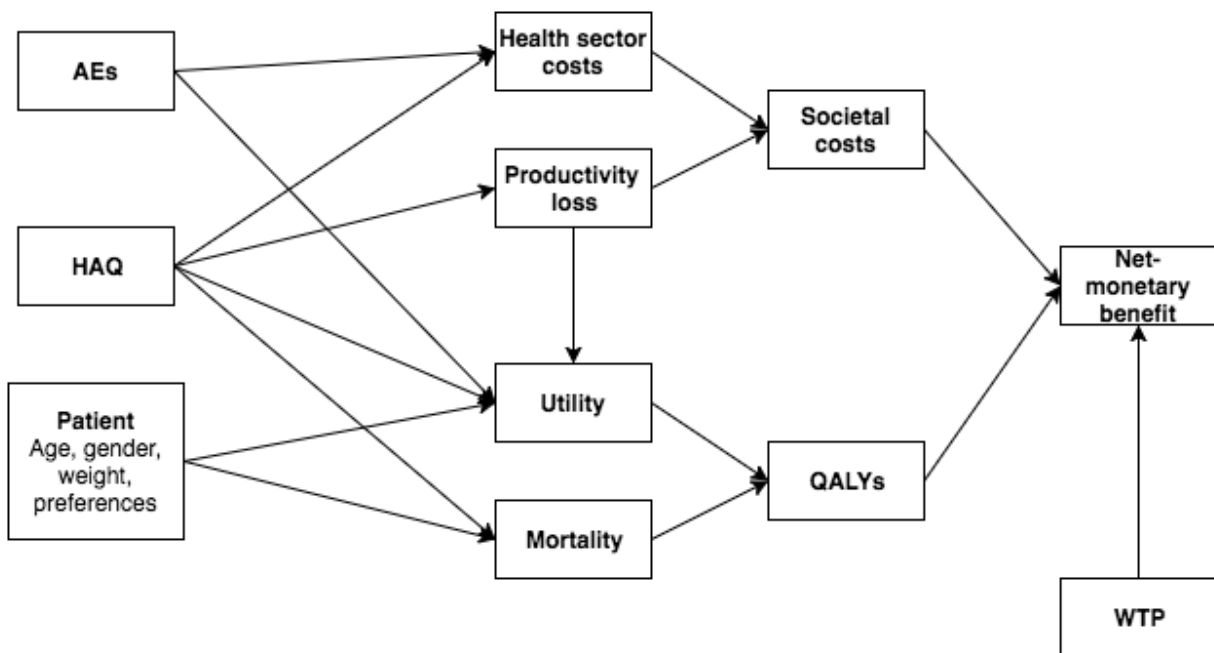
(b) Model outcomes

Figure 3: Influence diagram outlining structural relationships

Notes: ACR: American College of Rheumatology; EULAR: European League Against Rheumatism; HAQ: Health Assessment Questionnaire; QALY: AEs: adverse events; QALYs: quality-adjusted life-years; WTP: willingness to pay. Disease activity refers to the Disease Activity Score with 28-joint counts (DAS28) or the Simplified Disease Activity Index (SDAI).

Table 2: Competing model structures

Component of model structure	Possible combinations
Initial effect of treatment on HAQ (**H1-H3**) and switching (**S1-S6**)	12
HAQ trajectory	2
Probability distribution for treatment duration	7
Utility algorithm	2

4 Populations

To run the IPS, a patient population must be specified. The model is designed for patients who are cDMARD experienced. The patient characteristics that must be included in the analysis are age, HAQ, gender, weight, disease duration (in months), the number of previous DMARDs, and disease activity. These variables are measured at the start of the simulation (i.e., model cycle 0).

Two default options for the patient population are available. First, a homogeneous cohort of men and women with gender-specific weights but otherwise identical characteristics can be used. Second, a heterogeneous cohort of patients with gender-specific weights but varying across all other characteristics can be specified. Other populations (i.e., for certain subgroups or based on registry data) can be used as well but are not prespecified in our R package.

Our default population consists of individuals that, on average, have high disease activity. The proportion that is female, age, disease duration, the number of previous DMARDs, baseline HAQ, and DAS28 are based on the values reported in Curtis et al. (2010). Mean values for the SDAI and CDAI are from the US301 clinical trial—which had a DAS28 score similar to the value from Curtis et al. (2010)—summarized in Smolen et al. (2003). Summaries of each variable are reported in **??**. Details on the algorithm for simulating heterogeneous paients are described in Appendix B.

Table 3: Default inputs for patient population

	Mean	Standard deviation	Minimum	Maximum
Age	55.00	13.00	18	85
Male	0.21	-	-	-
Female weight (kg)	75.00	-	-	-
Male weight (kg)	89.00	-	-	-
Disease duration	18.65	12.25	0	-
Previous DMARDs	3.28	1.72	0	-
DAS28	6.00	1.20	0	9.4
SDAI	43.00	13.00	0	86
CDAI	41.00	13.00	0	76
HAQ	1.50	0.70	0	3

5 Source data and parameter estimation

5.1 Comparative treatment efficacy from NMA

The effects of treatment on ACR response, DAS28, and HAQ at 6 months are estimated using Bayesian network meta-analyses (NMA) of published randomized controlled trials (RCTs). Primary outcomes were ACR response, change in DAS28 from baseline at 6 months, and the change in HAQ from baseline at 6 months. Details of the methodology are provided in the Appendix (**??**).

Table 4: NMA estimates of ACR response, change in DAS28, and change in HAQ for biologic naive patients

	ACR response			ΔDAS28	ΔHAQ
	ACR20	ACR50	ACR70		
cDMARDs	0.263 (0.247, 0.280)	0.101 (0.093, 0.111)	0.032 (0.028, 0.036)	-1.149 (-1.218, -1.077)	-0.232 (-0.253, -0.212)
ABT IV + MTX	0.560 (0.471, 0.650)	0.313 (0.236, 0.399)	0.143 (0.097, 0.201)	-2.261 (-2.671, -1.870)	-0.447 (-0.572, -0.320)
ADA + MTX	0.562 (0.487, 0.637)	0.315 (0.249, 0.384)	0.144 (0.104, 0.193)	-	-0.555 (-0.674, -0.437)
ETN + MTX	0.646 (0.525, 0.761)	0.398 (0.280, 0.527)	0.202 (0.123, 0.303)	-2.655 (-3.244, -2.074)	-0.529 (-0.658, -0.399)
GOL + MTX	0.595 (0.437, 0.736)	0.349 (0.212, 0.497)	0.168 (0.084, 0.277)	-2.605 (-3.261, -1.964)	-0.499 (-0.625, -0.374)
IFX + MTX	0.663 (0.415, 0.872)	0.427 (0.195, 0.688)	0.232 (0.074, 0.459)	-1.939 (-2.480, -1.352)	-0.444 (-0.618, -0.258)
TCZ + MTX	0.555 (0.362, 0.739)	0.314 (0.159, 0.499)	0.147 (0.056, 0.280)	-3.004 (-3.300, -2.701)	-0.499 (-0.596, -0.402)
CZP + MTX	0.302 (0.095, 0.564)	0.131 (0.026, 0.317)	0.048 (0.006, 0.146)	-3.143 (-3.534, -2.719)	-0.556 (-0.662, -0.450)
ABT SC + MTX	0.568 (0.425, 0.705)	0.322 (0.202, 0.457)	0.150 (0.078, 0.245)	-2.266 (-2.946, -1.580)	-0.436 (-0.639, -0.236)
RTX + MTX	0.564 (0.409, 0.712)	0.320 (0.193, 0.470)	0.149 (0.073, 0.254)	-2.499 (-2.974, -2.053)	-0.516 (-0.629, -0.401)
TOF + MTX	0.591 (0.414, 0.756)	0.346 (0.195, 0.522)	0.168 (0.075, 0.298)	-	-0.464 (-0.689, -0.230)

Notes: ACR20/50/70 categories are the probability of at least a 20/50/70% improvement. 95% credible intervals are in parentheses. Estimates are based on 1,000 random draws of the NMA parameters. ΔDAS28 and ΔHAQ are changes in the DAS28 and HAQ score from their baseline scores respectively; negative numbers denote reductions in baseline values. cDMARDs = conventional disease-modifying antirheumatic drugs; MTX = methotrexate; ABT IV = abatacept intravenous; ADA = adalimumab; ETN = etanercept; GOL = golimumab; IFX = infliximab; TCZ = tocilizumab; CZP = certolizumab pegol; ABT SC = abatacept subcutaneous; RTX = rituximab; TOF = tofacitinib. ACR = American College of Rheumatology.

5.2 Treatment switching at 6 months

5.2.1 ACR response and change in disease activity

There are currently no established mappings between mutually exclusive ACR response categories and DAS28, SDAI, or CDAI (Madan et al. 2015). However, Aletaha and Smolen (2005) provides evidence on the relationship between overlapping ACR response categories (ACR 20/50/70) and mean changes in each of the three disease activity measures. Results are reported for three cohorts— the Leflunomide datasets, the inception cohort, and the routine cohort—with 1,839, 91, and 279 patients respectively. We transformed mean changes by overlapping ACR response categories to mean changes by mutually exclusive ACR response categories (ACR < 20, ACR 20-50, ACR 50-70, ACR 70+) by using the number of patients in each mutually exclusive ACR response category as described in Appendix C. Smolen et al. (2003) provided the number of patients in each ACR response category in the Leflunomide dataset and Aletaha et al. (2005) provided the number of patients in the inception cohort. Mean changes in each mutually exclusive ACR response category are shown in Table 5.

Table 5: Relationship between ACR response and change in disease activity measures

ACR response	Mean change at 6 months			
	Leflunomide dataset	Inception cohort		
	SDAI	SDAI	CDAI	DAS28
<20	0.000	0.000	0.000	0.000
20-50	-30.284	-13.700	-11.300	-1.550
50-70	-35.234	-14.882	-12.873	-1.543
70+	-41.000	-30.100	-27.600	-3.310

We did not include estimates from the routine cohort for two reasons. First, we were unable to find information on the number of patients in each ACR response category. Second, patients in the routine cohort had considerably lower disease activity levels (Aletaha and Smolen 2005; Aletaha et al. 2005) and our main population of interest (see Section 4) consists of patients with high disease activity at baseline. Mean DAS28 in the inception cohort and routine cohort were 5.62, and 4.09 respectively, while the mean DAS 28 ranged from 6.3 to 7 across the clinical trials making up the Leflunomide dataset.

5.2.2 ACR response and change in EULAR response

ACR responses were translated into EULAR response probabilities based on evidence of their relationship reported in Stevenson et al. (2016) and obtained from the US Veterans Affairs Rheumatoid Arthritis (VARA) registry (Table 6).

5.2.3 Probability of switching treatment

The probability of stopping treatment depends on the model structure used. If **S1** or **S6** is used, then patients stop treatment when there is no ACR response or no EULAR response, and continue treatment otherwise. If switching depends on SDAI, CDAI, or DAS28, then we model the probability of treatment switching and adjust it according to the level of disease activity.

Table 6: Relationship between ACR response and EULAR response

ACR response	EULAR response		
	None	Moderate	Good
<20	755	136	57
20-50	4	27	26
50-70	2	2	10
70+	0	2	2

Notes: The VARA registry is a multicentre, US database of veterans age 19 and older. Each cell represents the number of patients in the database in a given category.

Table 7: Coefficients from a logistic regression of the probability of switching treatment at 6 months

		95% CI	
Variable	Estimate	Lower	Upper
Intercept	-2.299	-2.329	-2.269
CDAI <10 (low)	0.000	0.000	0.000
CDAI 10-22 (moderate)	0.663	0.307	1.012
CDAI ≥ 22	1.221	0.820	1.621

Notes: Coefficients are log odds ratios. CDAI <10 (low) is a reference category.

The probability of treatment switching is estimated using a logistic regression equation. Differences in discontinuation by disease activity level are based on the odds ratios reported in Zhang et al. (2011) from an analysis of the Consortium of Rheumatology Researchers of North America (CORRONA) database. Zhang et al. (2011) estimated odds ratios for three disease activity categories based on CDAI (<10 (low), 10-22 (moderate), and ≥ 22 (high)). We set the intercept in our logistic regression equation so that the probability of treatment switching for a patient with moderate disease activity is 16.3%. This assumption is based on an estimate of the probability of treatment discontinuation at 6 months from a Kaplan-Meier curve estimated using the Consortium of Rheumatology Researchers of North America (CORRONA) database (see Section 5.6.1 for more details)—a population that tended to have moderate disease activity (mean CDAI = 16.0)—and is consistent with ranges from the literature (Souto et al. 2015). The standard error of the intercept was set so that the probability of switching with moderate disease activity varied by ± 3%. The coefficients for all variables in the logistic regression equations are shown in Table 7.

In the IPS, we use the absolute level of disease activity at 6 months (not at baseline) to make predictions. We define low, moderate, and high disease activity when using DAS28 and SDAI as in Anderson et al. (2012). The predicted probabilities of switching at 6 months for low, medium and high disease activity patients are 9.1%, 16.3%, and 25.4% respectively.

5.3 Change in HAQ at 6 months

As in Institute for Clinical and Economic Review (2017), ACR responses from the NMA were translated into HAQ scores based on evidence from the ADACTA trial reported in Carlson et al. (2015) (Table 8).

Table 8: Relationship between ACR response and change in HAQ at 6 months

| ACR response | HAQ change | |
	Mean	Standard error
<20	-0.11	0.06765
20-50	-0.44	0.05657
50-70	-0.76	0.09059
70+	-1.07	0.07489

Source: Carlson et al. (2015)

The relationship between EULAR response and HAQ is based on analyses conducted by Stevenson et al. (2016) using the BSRBR database. Their analysis is based on predictions from a mixture model with covariates set to sample means. Moderate and good EULAR responses are associated with -0.317 (SE = 0.048) and -0.672 (SE = 0.112) changes in HAQ scores respectively (Table 9).

Table 9: Relationship between EULAR response and HAQ

EULAR response	Mean	SE
None	0.000	0.000
Moderate	-0.317	0.048
Good	-0.672	0.112

Table 10 compares the impact of treatment on HAQ using model structures **H1-H3**.

Table 10: Simulated change in HAQ at 6 months under different model structures

	H1 ΔHAQ	H2 ΔHAQ	H3 EULAR no response	EULAR moderate response	EULAR good response	ΔHAQ
cDMARDs			0.61 (0.57, 0.65)	0.21 (0.17, 0.26)	0.18 (0.15, 0.23)	-0.19 (-0.81, 0.00)
ABT IV + MTX			0.39 (0.31, 0.47)	0.28 (0.20, 0.37)	0.33 (0.24, 0.44)	-0.31 (-0.84, 0.00)
ADA + MTX			0.39 (0.31, 0.47)	0.28 (0.19, 0.37)	0.33 (0.24, 0.44)	-0.31 (-0.84, 0.00)
ETN + MTX			0.33 (0.22, 0.43)	0.30 (0.20, 0.41)	0.38 (0.26, 0.52)	-0.35 (-0.85, 0.00)
GOL + MTX			0.37 (0.25, 0.48)	0.28 (0.20, 0.39)	0.35 (0.24, 0.49)	-0.33 (-0.85, 0.00)
IFX + MTX			0.31 (0.13, 0.50)	0.31 (0.20, 0.49)	0.38 (0.24, 0.58)	-0.35 (-0.85, 0.00)
TCZ + MTX			0.39 (0.25, 0.54)	0.27 (0.19, 0.39)	0.33 (0.22, 0.48)	-0.31 (-0.84, 0.00)
CZP + MTX			0.57 (0.37, 0.72)	0.22 (0.16, 0.30)	0.21 (0.11, 0.36)	-0.21 (-0.81, 0.00)
ABT SC + MTX			0.39 (0.28, 0.51)	0.28 (0.20, 0.38)	0.33 (0.23, 0.47)	-0.31 (-0.84, 0.00)
RTX + MTX			0.38 (0.27, 0.51)	0.28 (0.19, 0.39)	0.34 (0.23, 0.46)	-0.32 (-0.84, 0.00)
TOF + MTX			0.36 (0.23, 0.50)	0.28 (0.20, 0.40)	0.35 (0.24, 0.50)	-0.33 (-0.85, 0.00)

Notes: 95% credible intervals are in parentheses. Estimates are based on 6-month simulations of 1,000 patients and 1,000 parameters sets for each therapy. ΔHAQ denotes a change in the HAQ score at 6 months from baseline; a negative value indicates a reduction in the HAQ score. cDMARDs = conventional disease-modifying antirheumatic drugs; MTX = methotrexate; ABT IV = abatacept intravenous; ADA = adalimumab; ETN = etanercept; GOL = golimumab; IFX = infliximab; TCZ = tocilizumab; CZP = certolizumab pegol; ABT SC = abatacept subcutaneous; RTX = rituximab; TOF = tofacitinib. ACR = American College of Rheumatology.

5.4 HAQ progression in the absence of bDMARD treatment

The natural course of HAQ progression in the absence of bDMARDs develops over time according to an estimated natural course for patients remaining on cDMARDs or following discontinuation of the last bDMARD of the sequence. The natural course of HAQ can either be assumed to change at a constant linear rate or be modeled using a non-linear mixture model.

5.4.1 Constant linear rate of progression

The rate of progression in the linear case is based on the observational study by Wolfe and Michaud (2010). They assessed the development of HAQ over time at six month intervals for up to 11 years among 3,829 RA patients who switched from non-biologic treatment to biologic treatment and participated in the National Data Bank for Rheumatic Diseases (NDB) longitudinal study of RA outcomes. The annual HAQ progression rate prior to biologic therapy was 0.031 (95% confidence interval (95%CI): 0.026 to 0.036) and is assumed to reflect the course of progression of HAQ in the absence of bDMARD.

Based on the same data, Michaud et al. (2011) reported overall and age-specific specific HAQ progression rates. The differences between the overall and age specific rates are as follows: <40: -0.020 (95%CI: -0.0223 to -0.0177); 40-64: -0.008 (95%CI: -0.0101 to -0.0059); $\geq$ 65 0.017 (95%CI: 0.0136 to 0.0204). These estimates are applied to the overall progression rate of 0.031 to obtain age specific HAQ progression rates (see Section D.1).

Table 11: Annual linear progression of HAQ in the absence of bDMARDs beyond 6 months

		95% CI		
	Estimate	Lower	Upper	Reference
Overall progression rate				
MTX or non-biologic treatment	0.031	0.026	0.036	Wolfe and Michaud (2010)
Change in overall progression rate by age				
<40	-0.020	-0.028	-0.012	Michaud et al. (2011)
40-64	-0.008	-0.010	-0.006	Michaud et al. (2011)
65+	0.017	0.013	0.021	Michaud et al. (2011)

Notes: 95% confidence intervals are calculated using a normal distribution. Confidence intervals for changes in HAQ progression rates by age assume no covariance between the overall progression rate and the age-specific rates reported by Michaud et al. (2011).

5.4.2 Latent class growth model

We also model the rate of HAQ progression using a mixture model approach that has increasingly been used to model HAQ progression over time (Stevenson et al. 2016; Norton et al. 2013, 2014). These models suggest that different subgroups have distinct HAQ trajectories and that the rate of worsening of HAQ progression decreases over time. We use the LCGM estimated by Norton et al. (2014) and since we aim to model trajectories for cDMARDs and NBTs we chose the specification based on data from the Early Rheumatoid Arthritis Cohort Study (ERAS) cohort, which has a high percentage of patients receiving methotrexate and a very small percentage receiving biologics. Complete details of the LCGM are provided in Section D.2.

The Norton et al. (2014) LCGM determined that there are four classes of patients and thus four distinct HAQ trajectories. The probability of class membership depends on 7 variables: age, gender,

DAS28, disease duration, rheumatoid factor, the ACR 1987 criteria for RA, and a measure of socioeconomic status. Age, gender, and the DAS28 are relevant to the way the population is defined within our model (see Section 4) and are therefore important determinants of the HAQ trajectory. Other variables (disease duration, rheumatoid factor, ACR criteria, and socioeconomic status) are not defined within our population. We consequently set disease duration (8.2 months), rheumatoid factor (0.73), and the socioeconomic status variable (0.49) equal to their mean values with the ERAS cohort. The ACR criteria was set to 1.

HAQ trajectores (in levels) by class are shown Figure 4. The dotted lines plot observed mean values. There are clear distinguishable classes as both the level of the HAQ score and its slope vary between groups. Norton et al. (2014) refer to the groups as "low", "moderate", "high", and "severe" groups, in order from the lowest HAQ scores to the highest. The observed trends for the low, medium, and high groups follow a J-shaped pattern with a sharp drop following treatment initiation and an upward slope thereafter, while the severe group experiences persistently high HAQ scores. Since our model separates the initial treatment phase from the maintenance phase, we are only concerned with HAQ progression following the iniital drop. As in Stevenson et al. (2016), we consequently only predict values from year 2 onward. The fitted values are the solid upward sloping lines in the plot.
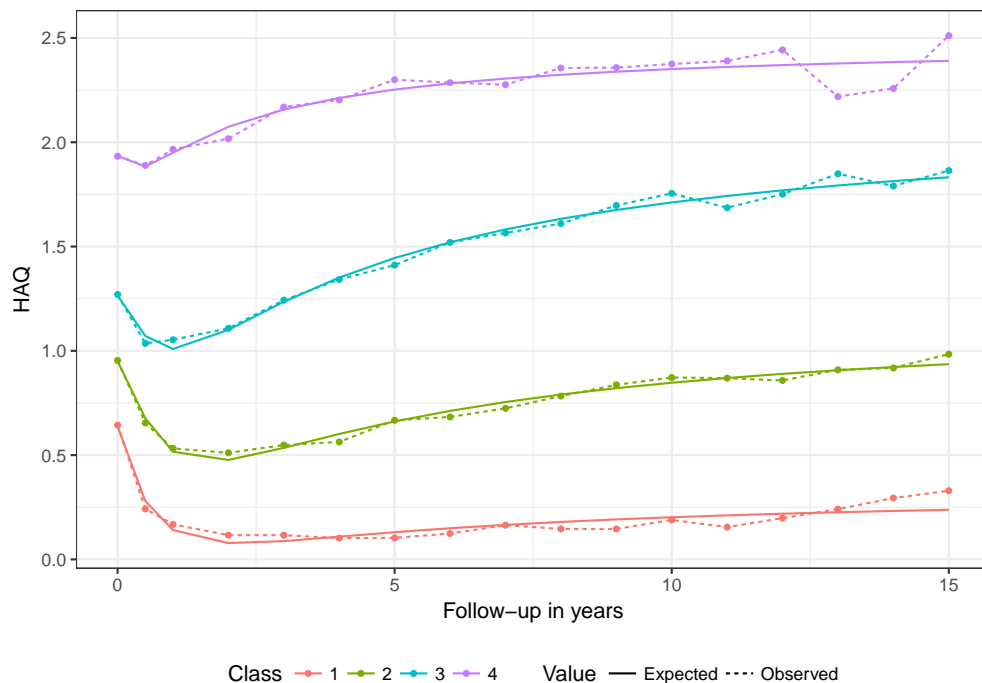
Figure 4: Observed and predicted HAQ trajectories in the ERAS dataset from the latent class growth model

An important question for cost-effectiveness modeling in RA is how the rate of progression within each class in the LCGM compares to a constant linear trajectory. We examine this question in Figure 5, which compares yearly rates of changes in HAQ using the LCGM and with constant annual rates of change (0.031 per year) based on the Wolfe and Michaud (2010) analysis. The LCGM was simulated over 30 years and differences between year t and year $t-1$ were used to assess changes in HAQ score from one year to the next.
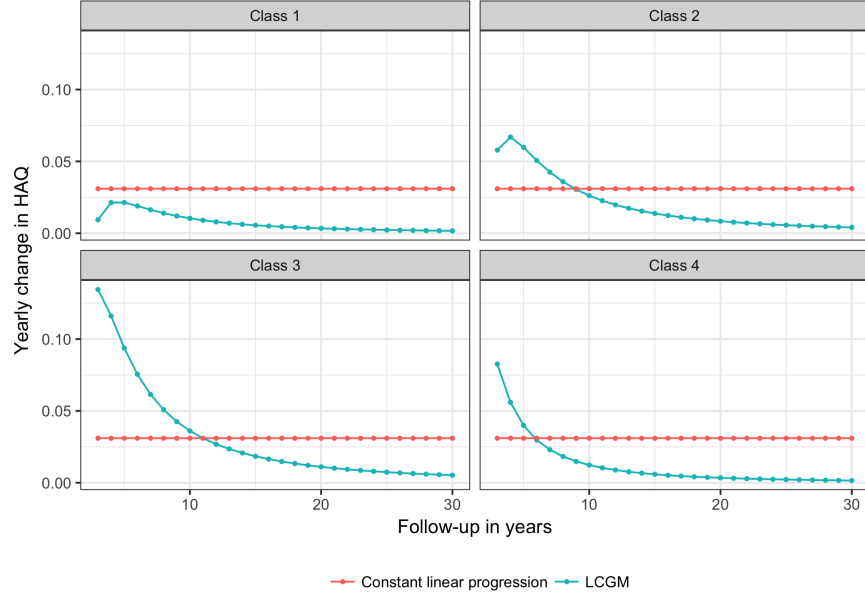
Figure 5: A comparison of predicted yearly changes in HAQ between a latent class growth model and constant linear progression from year 2 onwards

In the moderate, high, and severe groups the rate of HAQ progression is higher initialy in the LCGM than in the Wolfe and Michaud (2010) analysis; however, the LCGM modeled rate of HAQ progression declines over time and eventually begins to approach zero. In the low group, HAQ increases at a rate less than 0.031 per year and the rate of increase declines over time.

5.5   HAQ trajectory with bDMARD maintenance treatment

Based on the NDB longitudinal study, Wolfe and Michaud (2010) estimated the overall annual HAQ progression rate among RA patients who had switched to biologic treatment at -0.001 (95CI: -0.004 to 0.002). In a separate analysis, also based on NDB data, Michaud et al. (2011) reported annual HAQ progression rates by treatment adjusted for baseline HAQ score, age, sex, education, smoking, BMI, comorbidity, and RA onset. The average HAQ rate among patients on a biologic was -0.001 as well, which instills confidence that the reported HAQ progression rates for different bDMARDs as reported by Michaud et al. (2011) can be directly compared with the overall annual HAQ progression rate of 0.031 reported by Wolfe and Michaud (2010). Accordingly, bDMARD specific HAQ progression rates by Michaud et al. (2011) are used in the model. For bDMARD treatments evaluated in the model for which no HAQ progression rate was reported by Michaud et al. (2011), the overall biologic rate of -0.001 is used.

5.6   Duration of maintenance treatment

5.6.1   CORRONA database

Time to treatment discontinuation for patients on maintenance treatment for model structures **S1-S5** is based on analyses from the CORRONA database (Strand et al. 2013). The analysis sample consisted of 6,209 patients age 18 or older treated between 2002 and 2011 receiving either TNF inhibitors or other bDMARDs. The mean age was 57.6 years, 43% of patients were biologic naive, the mean CDAI was 16, and just over 26% of patients had high disease activity (CDAI $\geq$ 22).

7 parametric survival models (exponential, Weibull, Gompertz, gamma, log-logistic, lognormal, and generalized gamma) were estimated on individual patient data reconstructed from a Kaplan-Meier curve from the CORRONA analysis using the algorithm developed in Guyot et al. (2012). We compared fit using the Akaike Information Criteria (AIK) and Bayesian Information Criteria (BIC) (Table 12). The generalized gamma had the lowest AIC and BIC, so we consider it to be the preferred model. A plot of of the generalized gamma distribution against the Kaplan-Meier curve is shown in Figure 6. As can be seen in the plot, the shape of the survival curve estimated using a generalized gamma distribution tracks the Kaplan-Meier curve closely.

Table 12: AIC and BIC for parametric models of treatment duration from the CORRONA database

Distribution	AIC	BIC
Exponential	33,240	33,246
Weibull	33,182	33,196
Gompertz	32,963	32,977
Gamma	33,222	33,236
Log-logistic	32,848	32,861
Lognormal	32,650	32,663
Generalized gamma	32,507	32,527
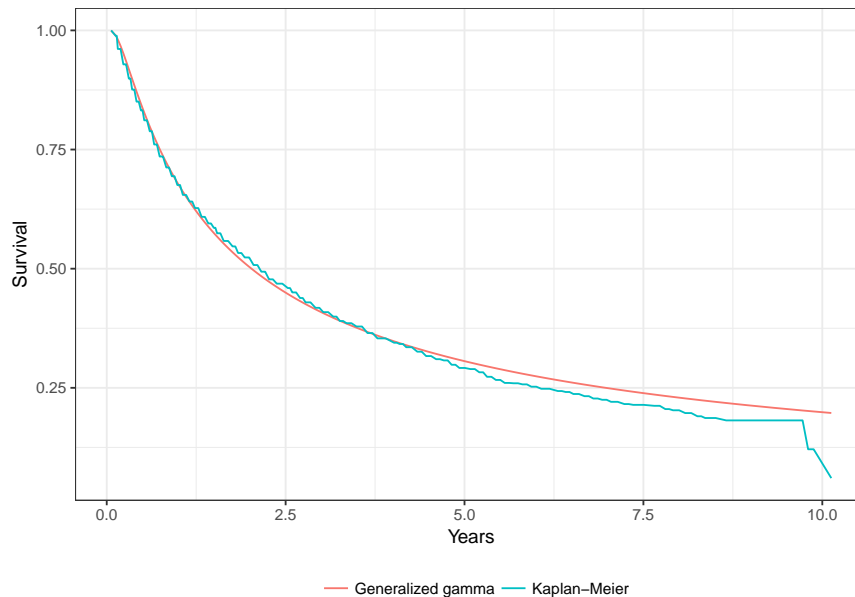
Figure 6: Generalized gamma and Kaplan-Meier time to treatment discontinuation curves using reconstructed individual patient data from the CORRONA database

We considered estimating separate time to discontinuation curves for each therapy, but did not for a number of the reasons cited in Stevenson et al. (2016). The majority of the literature focuses on anti-TNFs (e.g., infliximab, etanercept, and adalimumab) (e.g. Gomez-Reino and Carmona 2006; Yazici et al. 2009; Pan et al. 2009), which makes it difficult to estimate discontinuation curves

for the other therapies. Furthermore, studies comparing rates of discontinuation across therapies tend to be observational because clinical trials are of short duration and do not reflect real-world patient populations. However, although observational studies provide accurate predictions on time to discontinuation, it is difficult to avoid bias from confounding when estimating differences across treatments because patients are not randomized into treatment and control groups (Souto et al. 2015).

Unlike during the initial treatment phase, we do not condition rates of treatment discontinuation on the level of disease activity. The reason for this is that we could not find studies stratifying treatment duration curves by DAS28, SDAI, or CDAI. As a result, model structures **S1-S5** assume that conditional on continuing treatment beyond the first 6 months, duration does not depend on baseline disease activity, the change in disease activity from baseline, or whether the patient was biologic naive or experienced.

We also lack data on treatment duration for patients on cDMARDs. Following Stevenson et al. (2016), we assume that, conditional on continuing treatment at 6 months, treatment duration for bDMARDs is applicable to treatment duration for cDMARDs. This is, in turn, based on the assumption that cDMARDs are not likely to be more toxic than biologics used in combination with cDMARDs.

5.6.2 BSRBR database

In model structure **S6**, we stratify our time to treatment discontinuation by EULAR response based on analyses of the British Society for Rheumatology Biologics Registers (BSRBR) database (Stevenson et al. 2016). As with the CORRONA based estimates, we fit 7 parametric survival models using individual patient data reconstructed from survival curves using the Guyot et al. (2012) algorithm. We used the survival curves reported in Stevenson et al. (2016) to create the patient data. The Akaike Information Criteria (AIK) and Bayesian Information Criteria (BIC) of each model by EULAR response category (moderate, good) are shown in Table 13.

Table 13: AIC and BIC for parametric models of treatment duration by EULAR response

Distribution	Moderate EULAR response		Good EULAR response	
	AIC	BIC	AIC	BIC
Exponential	38,840	38,847	15,126	15,132
Weibull	38,478	38,492	15,090	15,101
Gompertz	38,099	38,112	15,066	15,077
Gamma	38,587	38,600	15,098	15,110
Log-logistic	38,142	38,155	15,062	15,073
Lognormal	37,988	38,001	15,047	15,059
Generalized gamma	37,869	37,889	15,048	15,065

One concern is that the BSRBR is representative of the UK but not the US. As a result, we also estimate "adjusted" survival models appropriate for US based analyses. The adjustment is made in six steps using the analyses from the CORRONA database described in Section 5.6.1.

1. Calculate a hazard function based on a survival curve from an analysis of the CORRONA database. In particular, reconstruct individual patient data from the survival curve Guyot

et al. (2012) and fit a spline-based survival model. Then use the spline-based model to estimate the hazard function $h(t)_{corrona}$.

2. Calculate a hazard function based on the BSRBR. To do so, first calculate hazard functions for both moderate and good EULAR responders using the same method described in step 1. Then calculate an overall hazard function with the proportion of moderate and good responders in the BSRBR analysis. Given that the number of moderate responders is $5{,}492$ and the number of good responders is $2{,}417$ the overall hazard function is $h(t)_{bsrbr} = \frac{5{,}492}{7{,}909} h(t)_{bsrbr,moderate} + \frac{2{,}417}{7{,}909} h(t)_{bbsrbr,good}$.

3. At each point in time, calculate the ratio of the CORRONA and BSRBR hazard functions: $HR(t) = h(t)_{corrona}/h(t)_{bbsrbr}$.

4. Apply the hazard ratio in step 3 to the BSRBR hazard functions for each EULAR response category. That is $h(t)_{bsrbr,moderate,adj} = h(t)_{bsrbr,moderate} \cdot HR(t)$ and $h(t)_{bsrbr,good,adj} = h(t)_{bsrbr,good} \cdot HR(t)$.

5. Generate survival curves using the hazard functions from step 4. Specifically, given a general hazard function $h(t)$, calculate the cumulative hazard functions, $H(t) = \int_{z=0}^{t} h(z)dz$, convert this to a survival function using $S(t) = exp(-H(t))$, and reconstruct individual patient data using the survival curve.

6. Fit parametric survival models to the individual patient data generated in step 5.

Both adjusted and unadjusted survival curves by EULAR response fit using a generalized gamma distribution are shown in Figure 7. AIC and BIC for the parametric models fit in step 6 do the adjusted individual patient data are shown in Table 14.

Table 14: AIC and BIC for CORRONA adjusted parametric models of treatment duration by EULAR response

Distribution	Moderate EULAR response		Good EULAR response	
	AIC	BIC	AIC	BIC
Exponential	42,304	42,310	18,098	18,103
Weibull	41,946	41,959	18,051	18,062
Gompertz	41,569	41,582	18,039	18,050
Gamma	42,098	42,111	18,063	18,074
Log-logistic	41,406	41,419	18,037	18,049
Lognormal	41,235	41,248	18,004	18,016
Generalized gamma	41,110	41,129	18,000	18,017

5.7 Rebound post treatment

Since no data exists on the size of the HAQ rebound post treatment, we vary its size as a proportion of the initial 6-month HAQ decline. 1 is used as an upper bound, which implies that the HAQ rebound is equal to the improvement experienced at the end of the initial 6-month period with that treatment. 0.5 is used as a lower bound based on expert opinion.
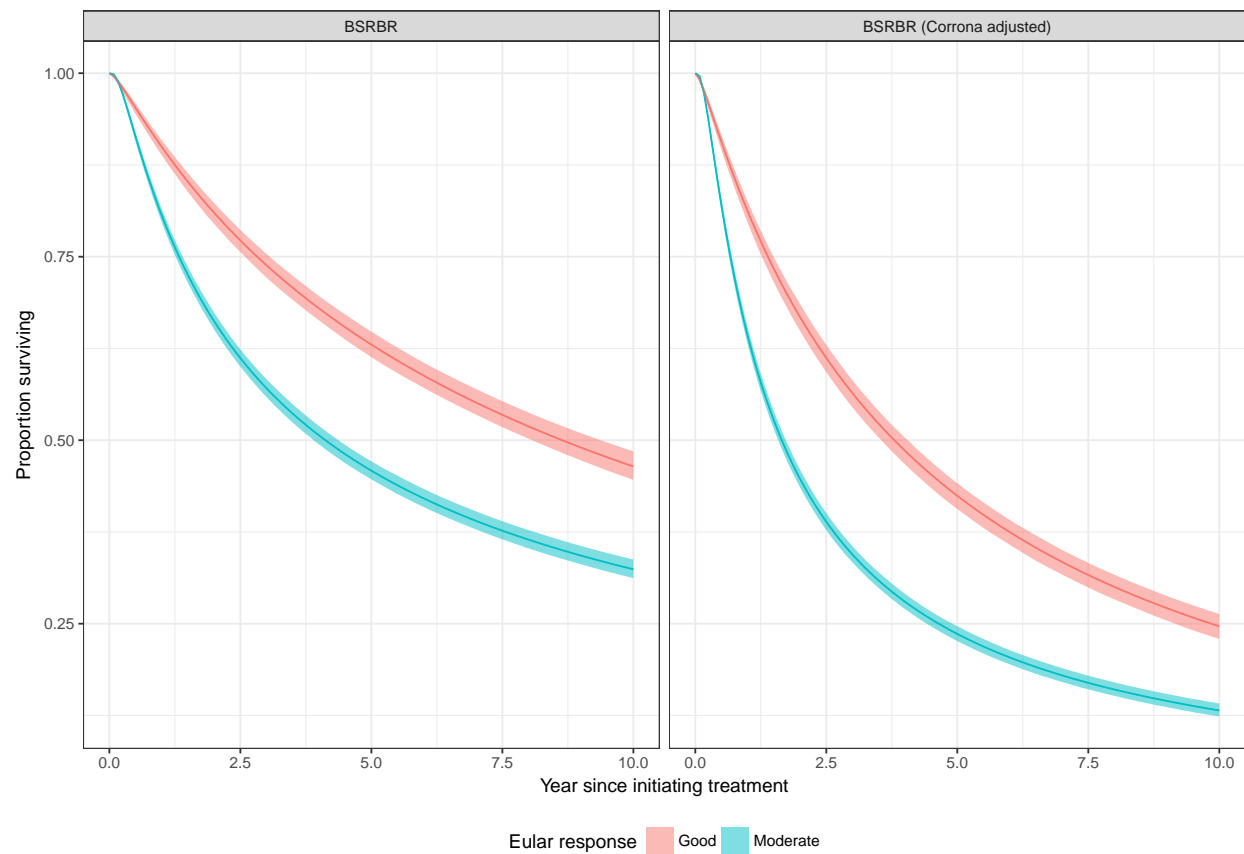
Figure 7: Generalized gamma survival curve of treatment duration using reconstructed individual patient data based on analyses from Stevenson et al. (2016) by EULAR response category

5.8 Serious infections

Based on the NMA by Singh et al. (2011) and in accordance with Stevenson et al. (2016), we assume a rate of 0.035 (95% CI: 0.027 to 0.046) infections per person-year with all bDMARDs and a rate of 0.026 (no CI reported) infections per person-year with cDMARDs. The rate of infection is assumed to be equal across bDMARDs because the published results for specific bDMARDs are estimated with very little precision. The standard error on the infection rate for bDMARDs is assumed to be the same as the standard error for cDMARDs since no standard error was reported for bDMARDs in Singh et al. (2011).

Table 15: Probability of serious infection

| | Probability | | |
| | | 95% CI | |
	Mean	Lower	Upper
cDMARDs or NBT	0.0574	0.0390	0.0790
bDMARDs	0.1116	0.0790	0.1480

Notes: Probabilities are estimated by simulating 1,000 patients and 1,000 parameter sets. Treatment duration is simulated using a generalized gamma distribution.

A patient in the IPS has a serious infection if a serious infection occurs before the simulated time of treatment discontinuation. Table 15 shows the probability of this occuring when treatment duration is modeled using a generalized gamma distribution. The probability of a serious infection is relatively rare as only 0.06 of patient on cDMARDs and 0.11 using bDMARDs have serious infections. However, differences between cDMARDs and bDMARDs are not insignificant as the probability of a serious infection is almost 5 percentage points higher with bDMARDs than with cDMARDs.

Table 16: Probability of serious infection with cDMARDs by distribution used to model treatment duration

Distribution	Mean probability
Exponential	0.0572
Weibull	0.0570
Gompertz	0.0575
Gamma	0.0573
Log-logistic	0.0578
Lognormal	0.0574
Generalized gamma	0.0574

Notes: Probabilities are estimated by simulating 1,000 patients and 1,000 parameter sets.

An important question related to the sensitivity of results to the model specification is whether the probability of serious infections depends on the distribution used to model time to treatment discontinuation. Table 16 consequently compares serious infection probabilities by the distribution used to simulate treatment duration. There are very small differences across distributions, suggest-

ing that the treatment duration distribution has almost no impact on the probability of serious infections.

5.9 Utility

Two algorithms can be used to map HAQ to an EQ-5D utility score. Each is used to simulate utility for every patient in the model to obtain a distribution of utility over time. Our preferred algorithm is the mixture model developed by Alava et al. (2013), which is described in detail in Appendix F. The second algorithm uses the logistic regression equation reported in Wailoo et al. (2006). The regression coefficients are shown in Table 17 and are used to predict utility with the inverse logit function (see Section A.1).

Table 17: Logistic regression coefficient from Wailoo utility algorithm

	Estimate	Standard error
Intercept	2.0734	0.0263
Age	0.0058	0.0004
Disease duration	0.0023	0.0004
Baseline HAQ	-0.2004	0.0101
Male	-0.2914	0.0118
Number of previous DMARDs	0.0249	0.0028
Current HAQ	-0.8647	0.0103

Notes: Coefficients are from the logistic regression reported in Wailoo et al. (2006).

Figure 8 compares results from the two algorithms. Mean utility scores from the Alava et al. (2013) mixture model lie above those from the Wailoo et al. (2006) equation for all values of HAQ. Moreover, the slope of utility curve produced from the mixture model is steeper (although less so for the commonly observed HAQ scores between 1 and 1.5), implying that changes in HAQ from the mixture model predict larger changes in utility. Given that the mixture models have been shown to predict utility more accurately (Alava et al. 2012, 2013; Hernández Alava et al. 2014), this suggests that standard models underestimate the quality-adjusted life-year benefits, and hence, the cost-effectiveness of treatments.

The utility score depends on two other factors in addition to HAQ. First, disutility due to serious infections is assumed to be 0.156 for the duration of the month of infection based on prior studies (Stevenson et al. 2016; Oppong et al. 2013). However, given the weak evidence for this estimate, the disutility of an infection is allowed to vary by 20% in either direction. Second, patient preferences for treatment unrelated to efficacy or serious infections (e.g., preferences for treatment attributes) can have a direct effect on utility. Given the limited evidence, we currently assume that this effect is 0, but have programmed the model so that preferences for treatment can easily be incorporated into the model if new evidence emerges.

5.10 Mortality

The probability of death is simulated as a function of age/sex specific mortality from U.S. lifetables (Arias 2015), baseline HAQ, and changes in HAQ from baseline. Wolfe et al. (2003) estimate an odds ratio for the effect of HAQ on mortality of 2.22, which is applied to the absolute mortality rates of the general population (HAQ score of 0). To capture the effect of treatment on mortality, we assume that, for every 0.25-unit increase in HAQ score, subsequent 6-month mortality increases
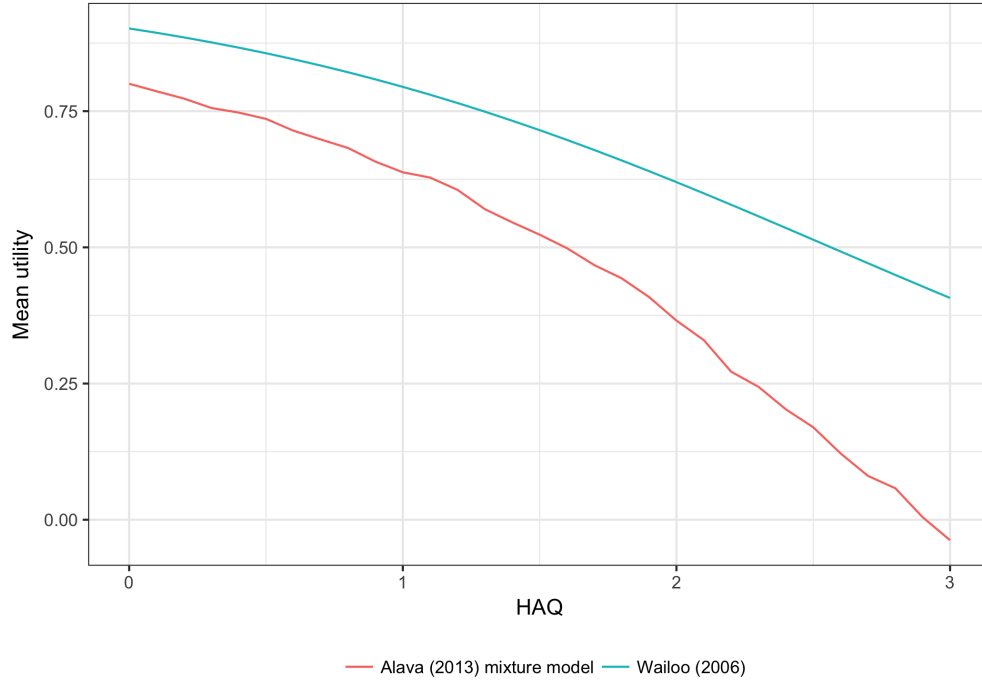
Figure 8: Simulated mean utility by current HAQ

according to the hazard ratios reported in Michaud et al. (2012). Parameter estimates are shown in Table 18.

Table 18: Mortality parameters

		95% CI		
	Estimate	Lower	Upper	Reference
Impact of baseline HAQ on mortality				
Log odds of mortality	0.798	0.582	1.012	Wolfe et al. (2003)
Impact of change in HAQ from baseline on mortality				
Log hazard ratio 0-6 months	0.113	0.077	0.157	Michaud et al. (2012)
Log hazard ratio >6-12 months	0.148	0.104	0.191	Michaud et al. (2012)
Log hazard ratio >12-24 months	0.148	0.095	0.191	Michaud et al. (2012)
Log hazard ratio >24-36 months	0.191	0.131	0.247	Michaud et al. (2012)
Log hazard ratio >36 months	0.174	0.104	0.239	Michaud et al. (2012)

Notes: 95% confidence intervals are calculated using normal distributions on the log odds and log hazard ratio scales.

Figure 9 plots survival curves by gender for 1,000 patients with a baseline age 55. Survival was simulated by setting the log odds ratios and log hazard ratios from tbl:mortpars equal to their point estimates. Three scenarios are considerd. In scenario one, patients do not have rheumatoid arthritis (i.e., HAQ score of 0). In the second scenario patients have baseline HAQ score of 1 but it does not increase over time. In the third scenario, patients still have a baseline HAQ score of 1 but it increases by 0.03 per year. The third scenario therefore utilizes the relationship between changes and HAQ and mortality from Michaud et al. (2012) while the second scenario does not.

Mean survival for females without RA was 82.5 years and declined to 77.0 for females with a constant baseline HAQ of 1 and to NaN when HAQ increased by 0.03 per year. Mean survival for males in

the first, second, and third scenario were 79.4, 73.2, and NaN years respectively. Overall, the figure suggests that RA increases mortality and that larger increases in HAQ over time increase mortality by even more.
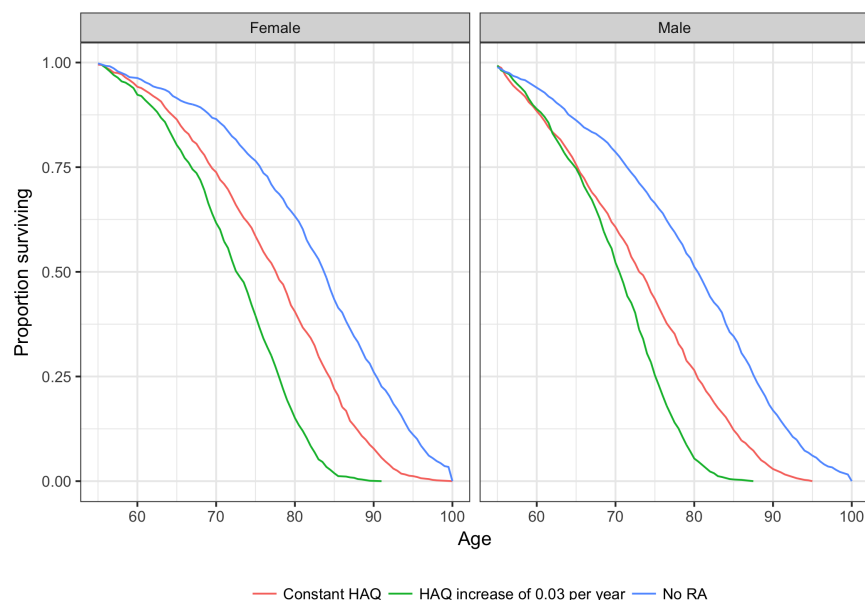
Figure 9: Simulated survival curve for a patient age 55

Notes: Baseline HAQ is 1 for the "Constant HAQ" and "HAQ increase of 0.03 per year" scenarios; baseline HAQ is 0 for the "No RA" scenario.

5.11   Cost

An overview of drug acquisition and administration costs is presented in Table 19. Costs are a function of dose and frequency of administration, strength and dosage form, the wholesale acquisition cost (WAC), and infusion costs. Since infliximab dosing depend on patient weight, the costs for infliximab reported in the table average over a patient population that is 21% male. The WACs in the table do not include discounts or rebates so they may be higher than actual drug costs.

Table 19: Drug acquisition and administration cost

Drug	Dose and frequency of administration	Strength and dosage form	Number of doses first 6 months	Number of dosees per year beyond the first 6 months	WAC per unit	Infusion cost	Cost for the first 6 months	Cost per year beyond the first 6 months
Etanercept	50 mg QW	50 mg/0.98 mL syringe or pen injector	26	52	1,110.50	0	28,873	57,746
Adalimumab	40 mg EOW	40 mg/0.8 mL syringe or pen injector	13	26	2,220.62	0	28,868	57,736
Infliximab	3 mg/kg at 0, 2, and 6 weeks, 3mg/kg Q8W, 6 mg/kg Q6W after 6 months	100 mg vial	5	8	1,113.27	164	17,519	51,853
Golimumab	50 mg QM	50 mg/0.5 mL syringe or pen injector	6	12	3,811.18	0	22,867	45,734
Certolizumab pegol	400 mg at weeks 0, 2, 4 then 200 mg Q2W	400 mg kit or syringe kit (200 mg 2)	8	26	3,679.87	0	29,438	47,838
Abatacept IV	750 mg IV at weeks 0, 2, 4 then Q4W	250mg vial	8	13	931.16	164	23,659	38,447
Abatacept SC	125 mg SC QW with IV loading dose	125mg/ml syringe	26	52	957.14	0	24,885	49,771
Tocilizumab	162 mg SC EOW	162 mg/0.9 mL syringe	13	26	898.31	0	11,678	23,356
Rituximab	1000 mg at weeks 0, 2; then Q24 W	500 mg/50ml vial	4	4	4,176.10	164	34,064	36,903
Tofaticinib citrate	5 mg BID	5mg tablet	364	728	63.26	0	23,026	46,053
Methotrexate monotherapy	15mg QW	15 mg injection	26	52	32.42	0	842	1,685
Hydroxychlorquine sulfate	400mg daily	200 mg tablet	182	364	3.18	0	1,157	2,315
Sulfazalazine	1-2 g daily	500 mg tablet	182	364	0.47	0	342	684

Notes: Costs do not include rebates or discounts. Cost for infliximab are calculated by assuming that 21% of patients are male and that the weight of men and women are 89 kg and 75 kg respectively. Tocilizumab is dosed weekly if weight is greater than 100 kg; costs for tocilizumab reported in the table are for patients weighing less than 100 kg. IV = intravenous; SC = subcutaneous; WAC = whoesale acqustion cost.

Parameters associated with resource use are showin in Table 20. Costs related to physician visits, chest X-rays, tuberculosis tests, and outpatient follow-up are based on Claxton et al. (2016). The cost per hospital day and the relationship between the HAQ score and the annual number of hospital days are from Carlson et al. (2015). Cost of any serious infection are assumed to be equal to the cost of pneumonia hospitalization at \$5,873, based on Medicare reimbursement rates. Wolfe et al. (2005) provide an estimate of annual income loss in relation to HAQ scores: \$4,372 (95% CI: 2,078 to 6,607; 2002 dollars) change per unit HAQ change, which are inflated to 2016 dollars.

Table 20: Resource use parameters

| | | 95% CI | | |
	Estimate	Lower	Upper	Reference
Days in hospital per year				
HAQ: 0-<0.5	0.260	0.000	1.725	Carlson et al. (2015)
HAQ: 0.5-<1	0.130	0.000	1.409	Carlson et al. (2015)
HAQ: 1-<1.5	0.510	0.015	1.850	Carlson et al. (2015)
HAQ: 1.5-<2	0.720	0.092	1.979	Carlson et al. (2015)
HAQ: 2-<2.5	1.860	1.013	2.960	Carlson et al. (2015)
HAQ: >2.5	4.160	3.238	5.196	Carlson et al. (2015)
Cost per day in hospital	1,251	904	1,652	Carlson et al. (2015)
General management cost				
Chest x-ray	109	97	121	Claxton et al. (2016)
X-ray visit	53	45	61	Claxton et al. (2016)
Outpatient follow-up	187	159	215	Claxton et al. (2016)
Mantoux tuberculin skin test	30	30	30	Claxton et al. (2016)
Productivity loss				
Linear regression coefficient - HAQ	5,853	2,861	8,845	Wolfe et al. (2005)

Notes: 95% confidence intervals for hospital days per year by HAQ score and hospital cost per day are calculated by using the methods of moments to generate the parameters of the gamma distribution given a mean and standard error. The 95% confidence intervals for general management costs are based on normal distributions as assumed in Claxton et al. (2016). 95% confidence interval for productivity loss are calculated using a normal distribution and inflated to 2016 dollars.

6 Simulation and uncertainty analysis

6.1 Individual patient simulation

The IPS is a discrete-time simulation that simulates individual patients one at a time. Model cycle, denoted by t, were chosen to be 6-months long to be consistent with most RCT and real-world data evidence. Algorithm 1 describes the main components of the IPS for a single patient and a given treatment in a treatment sequence. The full simulation cycles through each treatment in a sequence and through each simulated patient.

6.2 Parameter uncertainty

Parameter uncertainty is quantified using PSA, which propagates uncertainty in the model input parameters throughout the model by randomly sampling the input parameters from their joint probability distribution (Baio and Dawid 2015; Claxton et al. 2005). Probability distributions are determined according to the distributional properties of the statistical estimates, which, in turn, depend on the statistical techniques used and the distributions of the underlying data. We, for the most part, use normal distributions for sample means, gamma distributions for right-skewed data (e.g., hospital costs), and Dirichlet distributions for multinomial data. The multivariate normal

Algorithm 1 Main components of the individual patient simulation
_____

1. **Initial treatment effect** $(t = 0)$

   (a) Simulate clinical response (SDAI or EULAR), time to serious infection T_{si}, and death.

      i. **If** no clinical response, **then** stop treatment. Treatment switch caused by a serious infection if time to serious infection occured during cycle 0 (i.e. $T_{si} = 0$). Change in HAQ is assumed to be 0.
         Else if clinical response, **then** continue treatment. Simulate change in HAQ and time to treatment discontinuation T.

      ii. **If** patient died, **then** move to next patient.

2. **Maintenance phase** (for $t > 0$ and $t \leq T$)

   (a) Simulate death (see Appendix E) and change in HAQ.

   (b) **If** patient died, **then** move to next patient.

   (c) **If** $t = T$, **then** switch treatment. Treatment switch caused by a serious infection if time to serious infection occured during or before cycle T (i.e. $T_{si} \leq T$).
_____

distribution is used for regression parameters estimated using frequentist techniques, provided that the variance-covariance from the statistical analysis is available. For parameters estimated using a Bayesian statistical model, we use the posterior distribution generated from the Markov-Chain Monte-Carlo (MCMC) algorithm. When we lack evidence on a parameter, we typically assume a uniform distribution with lower and upper limits that reflect the degree of uncertainty in the parameter. The PSA parameter distributions are summarized in Table 21.

6.3 Structural uncertainty

We consider structural uncertainty due to two factors:

- The relationhip between health states within the model.

- The statistical model used to estimate parameters.

Both sources of uncertainty are reflected in Table 2. The choice of model structure for the initial treatment phase (**H1-H3** and **S1-S6**) depends on the preferred measures of disease included in the model as well as whether statistical relationships should be modeled directly or indirectly. Likewise, the choice of model for HAQ progression, treatment duration, and converting HAQ to utility all reflect uncertainty in the appropriate statistical model.

6.4 Implementation

We begin by describing the simulation procedure conditional on model structure, which uses PSA to capture uncertainty within but not between models. The procedure proceeds in two steps: first, model parameters are sampled from their joint probability distribution (Section 6.2), and second, for each parameter set, model outcomes are simulated one at a time for individual patients in the specified population (Section 4).

Table 21: Probabilistic Sensitivity Analysis Parameter Distributions

Parameter(s)	Distribution
Rebound factor	Uniform
NMA parameters - ACR response	Bayesian posterior distribution
NMA parameters - DAS28	Bayesian posterior distribution
NMA parameters - HAQ	Bayesian posterior distribution
Drug acquisition and administration cost	Fixed
Logistic regression coefficients for probability of treatment switch at 6 months	Normal
Survival model parameters for treatment duration during maintenance phase	Multivariate normal
US lifetable mortality rates	Fixed
Mortality probability odds ratio - baseline HAQ	Normal
Mortality probability hazard ratio - change in HAQ from baseline	Normal
ACR response to EULAR response mapping	Dirichlet
ACR response to SDAI mapping	Uniform
ACR response to CDAI mapping	Uniform
ACR response to HAQ mapping	Normal
EULAR response to HAQ mapping	Normal
Linear HAQ progression - by therapy	Normal
Linear HAQ progression - by age	Normal
Latent class growth model for HAQ progression	Normal
Utility model - Alava et al. (2013) mixture model	Multivariate normal
Utility model - Wailoo et al. (2006)	Normal
Hospital costs - hospital days by HAQ	Gamma
Hospital costs - hospital costs per day	Gamma
General management cost	Gamma
Serious infection - survival parameters	Normal
Serious infection - cost per infection	Uniform
Serious infection - utility loss	Uniform

Analysts who wish to expand the analysis to capture uncertainty between models can follow the approach described in Bojke et al. (2009). In particular, for each randomly sampled parameter set, each model structure (or a subset of plausible model structures) can be simulated. The distribution of simulated outcomes across parameters and models will then reflect uncertainty both within and between models.

Its important to note that simulation output for an individual patient captures differences in outcomes across patients due to random variation (often referred to as first order uncertainty). This information might be useful to patients since it is needed to predict the distribution of their future outcomes conditional on their characteristics, but less useful to a decision maker concerned with making treatment decisions for a population or subset of a population. Analysts wishing to use the model for CEA should therefore estimate mean outcomes by averaging over the simulated patients for each parameter set and model structure. The number of simulated patients should be sufficiently large so that mean outcomes are stable across model runs (i.e., first order uncertainty is eliminated).

Although CEA is concerned with mean outcomes, that does not imply that it does not account for heterogeneity. Instead, since outcomes depend on the characteristics of each patient, model averages are a function of the population analyzed. Subgroup analyses can be used to examine differences in cost-effectiveness across subgroups by simulating patients with certain shared characteristics.

Parameter and structural uncertainty imply decision uncertainty, or the degree to which decisions are made based on imperfect knowledge. Indeed, with the aim to maximize health outcomes for a given budget, the optimal decision with current information is to choose the policy that maximizes the expected NMB; however, due to uncertainty, the incorrect policy may be considered the most cost-effective. To characterize this uncertainty, standard summary measures including 95% credible intervals for NMBs and other model outcomes, cost-effectiveness planes, and cost-effectiveness acceptability curves, and the expected value of perfect information can be calculated from the simulated output. Since the expected value of partial perfect information is computationally costly, it can be approximated using meta-modeling techniques (Jalal et al. 2013, 2015; Heath et al. 2016).

Appendices

A Mathematical formulas

A.1 Predicted probabilities from a logistic regression

Predicted probabilities from logistic regressions are calculated using the inverse logit function,

$$\hat{p} = \frac{1}{1 + \exp(-x\beta)}, \tag{1}$$

where β is a vector of regression coefficients.

A.2 Using odds ratios to adjust probabilities

Let p_1 be a baseline probability, β be a vector of log odds ratios, and x be a vector of regressors. We apply the log odds ratios to p_1 to generate a new probability p_2 with the logistic equation,

$$p_2 = \frac{1}{1 + \exp\left[-\left(\text{logit}(p_1) + x^T\beta\right)\right]}, \tag{2}$$

where,

$$\text{logit}(p) = \log\left(\frac{p}{1-p}\right) \tag{3}$$

A.3 Converting rates and probabilities

Given a *constant* rate r during a given time period, we estimate the probability of an event ocurring before time t using the exponential distribution,

$$p(\tau < t|r) = 1 - e^{-rt}. \tag{4}$$

Given a probability p, the rate parameter is recovered by applying the log transformation,

$$r = \frac{-\ln(1-p)}{t}. \tag{5}$$

A.4 Calculating standard errors from confidence intervals

Journal articles often report confidence intervals rather than standard errors. However, given that regression coefficients are asymptotically normally distributed, standard errors can be calculated from a confidence interval using the normal distribution. In particular, given a coefficient estimate β (e.g., a log hazard ratio, log odds ratio, or linear regression coefficient) and an upper bound u and lower bound l of a two-sided 95% confidence interval, we calculate the standard error as,

$$SE(\beta) = \frac{u - l}{2 \cdot \Phi^{-1}(0.975)}, \tag{6}$$

where $\Phi^{-1}(p)$ is the quantile function of the normal distribution.

B Heterogeneous populations

When generating heterogeneous patient populations, we sample binary variables from binomial distributions, continuous uncorrelated variables from normal distributions, and continuous correlated variables from multivariate normal distributions. Truncated distributions are used when variables are restricted to lie within certain intervals. More specifically,the proportion of the female population is drawn from a binomial distribution while age, disease duration and the number of previous DMARDs are drawn from truncated normal distributions. Each sampled value of the number of

previous DMARDs is rounded to the nearest integer. Baseline HAQ and three disease activity measures (DAS28, SDAI, and CDAI) are drawn from truncated multivariate normal distributions. The covariance matrix is calculated using the correlations reported in Aletaha et al. (2005) (Figure 10).
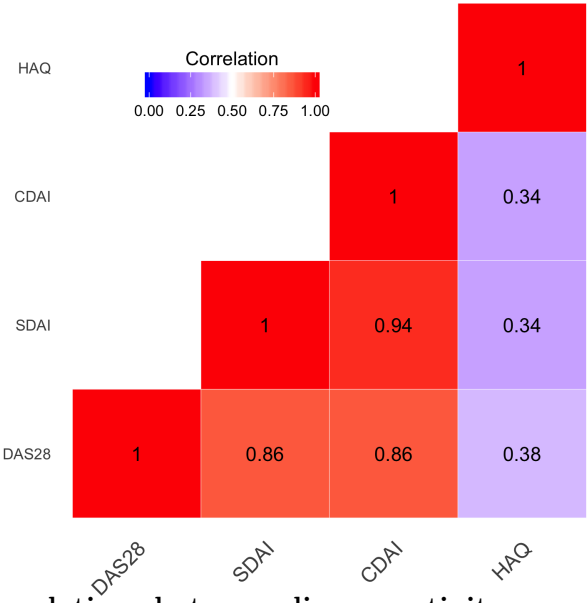
Figure 10: Correlations between disease activity measures and HAQ

We used the correlations from the routine cohort (during visit 1) rather than correlations in the inception cohort (at baseline) since the correlation between HAQ and the disease activity measures were more similar to those from the Leflunomide database (Smolen et al. 2003). That said, correlations between the three disease activity measures were nearly identical in each cohort. The one exception was that the correlation between SDAI and CDAI of 1 in the routine cohort seemed unreasonably high so we used the value of 0.94 from the inception cohort.

We used this sampling procedure to simulate 1,000 patients. Summary statistics from the simulated patient cohort are 1,000 are shown in Table 22.

Table 22: Summary of characteristics for 1,000 simulated patients

	Mean	95 CI% Lower	95 CI% Upper
Age	54.58	31.11	77.17
Male	0.21	0.00	1.00
Weight (kg)	78.01	75.00	89.00
Disease duration	20.06	2.60	43.35
Previous DMARDs	3.38	0.98	6.00
DAS28	5.98	3.81	8.09
SDAI	42.86	20.17	66.02
CDAI	40.99	16.61	63.89
HAQ	1.52	0.30	2.67

C   Mapping ACR response to changes in disease activity

Let DA denote disease activity, n_1 the number of patients with ACR 20-50 response, n_2 the number of patients with ACR 50-70 response, n_3 the number of patients with ACR 70 response, and N the number of patients with an ACR response greater than or equal to 20%. Mean changes in SDAI, CDAI, and DAS28 by overlapping ACR response categories are converted to mean changes by mutually exclusive ACR response categories as follows:

- **ACR 70**: Mean changes by ACR 70 were reported directly in Aletaha and Smolen (2005).

- **ACR 50-70**: Mean change in disease activity given ACR 50-70 response is calculated by solving for $\mathbb{E}[DA|50 \leq ACR < 70]$:

$$\mathbb{E}[DA|ACR \geq 50] = \frac{n_2}{N} \cdot \mathbb{E}[DA|50 \leq ACR < 70] + \frac{n_3}{N} \cdot \mathbb{E}[DA|ACR \geq 70] \tag{7}$$

- Mean change in disease activity given ACR 20-50 response is calculated by solving for $\mathbb{E}[DA|20 \leq ACR < 50]$

$$\mathbb{E}[DA|ACR \geq 20] = \frac{n_1}{N} \cdot \mathbb{E}[DA|20 \leq ACR < 50] + \frac{n_2 + n_3}{N} \cdot \mathbb{E}[DA|ACR \geq 50] \tag{8}$$

D   HAQ progression

D.1   Effect of age on linear HAQ progression

Michaud et al. (2011) report an overall rate of linear HAQ progression and rates for three age groups (<40, 40-64, $\geq$ 65). Let β be the overall rate of progression and β_a be the rate of progression for age group a. To estimate the effect of age on the progression rate, we calculated the difference between the overall progression rate and the age specific rate, $\delta_a = \beta - \beta_a$. We estimated the standard error of this quantity assuming no covariance between β and β_a,

$$SE(\delta_a) = \sqrt{SE(\beta)^2 + SE(\beta_a)^2}. \tag{9}$$

D.2 HAQ trajectory with a latent class growth model

Norton et al. (2014) model HAQ progression using a latent class growth model (LCGM). The probability that individual i is a member of class c at time t is modeled using a multinomial logistic regression,

$$P(C_{it} = c) = \frac{\exp(w_{it}^T \delta_c)}{\sum_{s=1}^{4} \exp(w_{it}^T \delta_s)}, \tag{10}$$

where δ_s is the vector of regression coefficients associated with class s and w_{it} is the corresponding vector of regressors. The variables included in w_{it} are age, gender, baseline DAS28, symptom duration, rheumatoid factor, ACR criteria, and socioeconomic status. Regression coefficients for classes 2-4 relative to class 1 are shown in Table 23. Older age and female gender are especially important predictors of membership in higher risk classes; a worse DAS28 score, rheumatoid factor positivity, fullfilment of the 1987 ACR criteria, lower socioeconomic status, and longer disease duration are also predictors of membership in classes with worse HAQ progression.

The HAQ trajectory for a given class can be written as,

$$y_{itc}^* = \beta_{0c} + \beta_{1c}x_t + \beta_{2c}x_t^2 + \beta_{3c}x_t^3 + \epsilon_{it} \tag{11}$$

$$y_{itc} = \begin{cases} 0 & \text{if } y_{itc}^* < 0 \\ y_{itc}^* & \text{if } 0 \le y_{itc}^* \le 3 \\ 3 & \text{if } y_{itc}^* > 3, \end{cases} \tag{12}$$

where y_{itc} is the HAQ score, x_t is a variable that is a function of time, the β_{jc} are polynomial regression coefficients for members of class c, and ϵ_{it} is an error term.

Sam Norton generously provided us with statistical estimates of the 4 class LCGM used in Norton et al. (2014) from MPlus. Like Stevenson et al. (2016), we noted that the coefficient estimates the MPlus resulted in large fluctuations in the predicted HAQ scores, likely because three decimal places was not precise enough for the cubic term in Equation 11. We consequently used the coefficient estimates to predict the probability of class membership—which are less likely to be influenced by the number of reported decimal places—but estimated Equation 11 using the observed HAQ values reported in Figure 2 in Norton et al. (2014). Morevoer, since we are only interested in the HAQ trajectory following the HAQ decline during the initial treatment phase, we limited our analyis to HAQ values from year 2 and onwards. Using the post year 2 data, we estimated eqn:lcgm-haq using separate linear regressions with cubic polynomials for each class (Table 24). Like Norton et al. (2014), we set x_t equal to a reciprocal transformation of time,

$$x_t = 1 - \frac{1}{t+1} \tag{13}$$

Table 23: Determinants of class membership in the ERAS cohort

		95% CI	
	Coefficient	Lower	Upper
Class 2: moderate			
Intercept	-3.496	-4.715	-2.277
Age at onset	0.025	0.011	0.039
Female gender	0.841	0.457	1.225
Disease duration (months)	0.304	0.147	0.461
DAS28 score	0.032	0.001	0.063
Rheumatoid factor positive	0.214	-0.251	0.679
ACR criteria for RA	0.278	-0.163	0.719
Socioeconomic status	0.993	0.276	1.710
Class 3: high			
Intercept	-6.686	-7.980	-5.392
Age at onset	0.037	0.023	0.051
Female gender	1.694	1.275	2.113
Disease duration (months)	0.573	0.424	0.722
DAS28 score	0.046	0.013	0.079
Rheumatoid factor positive	0.315	-0.175	0.805
ACR criteria for RA	0.413	-0.050	0.876
Socioeconomic status	1.119	0.449	1.789
Class 4: severe			
Intercept	-12.055	-14.215	-9.895
Age at onset	0.082	0.060	0.104
Female gender	1.976	1.449	2.503
Disease duration (months)	0.800	0.631	0.969
DAS28 score	0.042	0.001	0.083
Rheumatoid factor positive	0.298	-0.270	0.866
ACR criteria for RA	0.939	0.320	1.558
Socioeconomic status	1.429	0.682	2.176

Notes: Class 1, or the "low" group, is the reference category.

In the cost-effectiveness model, we simulate the HAQ score at 6 months as a function of the baseline HAQ score and the change in HAQ during the initial treatmment phase. Since the Norton et al. (2014) model is not conditional on the initial HAQ score (i.e., the simulated HAQ score at 6 months), we use it to predict changes in HAQ rather than the level of the HAQ score. More preciseley, for a patient in a given class, we model the change in HAQ as,

$$\Delta y_{itc}^* = y_{i,t,c}^* - y_{i,t-1,c}^* \qquad (14)$$
$$= \beta_{1c}(x_t - x_{t-1}) + \beta_{2c}(x_t^2 - x_{t-1}^2) + \beta_{3c}(x_t^3 - x_{t-1}^3) + (\epsilon_{i,t} - \epsilon_{i,t-1}).$$

Table 24: LCGM HAQ trajectory coefficients

	Coefficient	Standard error
Class 1: low		
Intercept	0.638	0.058
Linear	-1.009	0.074
Quadratic	-0.649	0.027
Cubic	1.355	0.003
Class 2: moderate		
Intercept	0.950	0.058
Linear	-0.109	0.020
Quadratic	-3.368	0.002
Cubic	3.699	0.064
Class 3: high		
Intercept	1.265	0.064
Linear	-0.132	0.056
Quadratic	-2.531	0.021
Cubic	3.538	0.002
Class 4: severe		
Intercept	1.935	0.063
Linear	-0.540	0.073
Quadratic	1.196	0.027
Cubic	-0.109	0.003

Notes: Class 1, or the "low" group, is the reference category.

Since Equation 11 was estimated on aggregated data, we did not have reliable estimates of ϵ_{it}. We consequently set $\epsilon_{i,t} - \epsilon_{i,t-1}$ equal to 0, which implies that we are generating a mean resopnse rather than a predicted response. In other words, we are not simulating the random variation associated with each individual, but are still accurately simulating mean outcomes accross populations or subpopulations.

E   Simulating death

Death is simulated for each patient during each model cycle based on age, gender, baseline HAQ, and change in HAQ from baseline. A 0/1 death indicator is randomly drawn using the following procedure:

1. Find q_{xg}, the probability that a patient of gender g and age x will die before age $x + 1$, from lifetables.

2. As described in Section A.2, adjust q_{gx} using the effect of a change in baseline HAQ on the odds of mortality, OR,

$$p_m = \frac{1}{1 + \exp\left[-(\text{logit}(q_x) + \log(OR) \cdot HAQ)\right]}. \tag{15}$$

3. Following Section A.3, convert the mortality probability, p_m, into a mortality rate, r_m.

$$r_m = -log(1 - p_m). \tag{16}$$

4. Adjust the mortality rate, r_m, using the estimated log hazard ratio of mortality, HR of a change in HAQ from baseline, Δ HAQ.

$$r_m = r_m \cdot \exp[\log(HR) \cdot \Delta HAQ] \tag{17}$$

5. Following Section A.3, convert the mortality rate into a probability given a 6-month cycle length,

$$p_m = 1 - \exp[-r_m * (6/12)]. \tag{18}$$

6. Randomly draw a 0/1 death indicator, d, given the probability of death, p_m,

$$d \sim \text{Bin}(1, p_m). \tag{19}$$

F   Simulating utility with a mixture model

The mixture model estimated by Alava et al. (2013) simulates utility in two stages. In the first stage, we sampled pain for a given individual in a particular model cycle based on the HAQ score. In the second stage, we simulated utility as a function of HAQ, pain and age/sex.

F.1   Simulating pain

To simulate pain from HAQ, we used the summary statistics for pain and HAQ reported in Sarzi-Puttini et al. (2002). Pain was measured with the visual analog scale (VAS) with mean $\mu_{pain} = 61.65$ and standard deviation $\sigma_{pain} = 19.10$, while HAQ was reported to have mean $\mu_{haq} = 1.39$ and standard deviation $\sigma_{haq} = 0.59$.

We then estimated the correlation between pain and HAQ by digitally scanning the curve depicting the (linear) relationship between pain and HAQ (Figure 114) shown in Stevenson et al. (2016). Using the scanned data, we regressed pain on HAQ using simple ordinary least squares (OLS). The correlation between pain and HAQ, estimated as $\rho = 0.52$, was calculated by rearranging the OLS estimate for the slope, β, of the regression model,

$$\rho = \beta \cdot \frac{\sigma_{haq}}{\sigma_{pain}}. \tag{20}$$

Pain was simulated using these parameters by assuming that pain was normally distributed conditional on HAQ,

$$pain|haq = h \sim N\left(\mu_{pain} + \rho\frac{\sigma_{pain}}{\sigma_{haq}}(h - \mu_{haq}), \sigma_{pain}^2(1 - \rho^2)\right). \tag{21}$$

However, since the VAS is constrained to lie between 0 and 100, pain was drawn from a truncated normal distribution with a lower limit of 0 and an upper limit of 100.

F.2 Simulating utility

After simulating pain, we simulated utility with a mixture model. Within each class c, the HAQ score for patient i in period t was modeled as,

$$y_{it|C_{it}} = \begin{cases} 1 & \text{if } y^*_{it|C_{it}} > 0.883 \\ y^*_{it|C_{it}} & \text{otherwise} \end{cases} \tag{22}$$

$$y^*_{it|C_{it}} = \alpha_{ic} + x_{it}^T \beta_c + \epsilon_{it} \tag{23}$$

$$\alpha_{ic} = \gamma_c + z_i^T \kappa + \mu_i, \tag{24}$$

where ϵ_{it} is a random error term and β_c is a vector of regression coefficients corresponding to the vector of variables x_{it}. α_{ic} is a random intercept for individual i and class c that is predicted by a class-specific intercept, γ_c, a vector of individual-specific variables z_i, a coefficient vector κ, and an error term, μ_i. Variables included in x_{it} are HAQ, HAQ^2, $Pain/100$, $Age/10$, and $Age/100$; z_i contains a single indicator variable, $Male$, equal to 1 if the patient is male and 0 if female.

The probability of class membership was modeled using a multinomial logit model,

$$P(C_{it} = c) = \frac{\exp(w_{it}^T \delta_c)}{\sum_{s=1}^4 \exp(w_{it}^T \delta_s)}, \tag{25}$$

where there are four possible classes and δ_c is a vector of coefficients correpsonding to the vector of variables, w_{it} (which includes an intercept). Variables included in w_{it} other than the intercept are HAQ, $Pain/100$, and $Pain/100^2$.

We sampled from the mixture model as follows.

1. For each individual i, sample the error term, $\mu_i \sim N(0, \sigma_\mu^2)$.

2. For each individual i and time-period t:

   (a) Sample class membership conditional on w_{it}; that is, sample $C_{it} \sim \text{Cat}(\text{p}_1, \text{p}_2, \text{p}_3, \text{p}_4)$ where p_c is the probability of being in class c.

   (b) Predict the intercept α_{ic}.

   (c) Sample the error term, $\epsilon_{it} \sim N(0, \sigma_\epsilon^2)$.

   (d) Predict the HAQ score, y_{it}.

G Network Meta-Analysis

G.1 Systematic literature review

Population

- Adult (>18 years) patients with moderate to severe RA who have had inadequate response to cDMARDs

Interventions and comparators

- Biologics as monotherapy or in combination with cDMARDs (adalimumab, certolizumab pegol, etanercept, golimumab, infliximab, abatacept, rituximab, tocilizumab, sarilumab, tofacitinib, baricitinib)

- Triple therapy (MTX, HCQ, and SSZ)

- cDMARDs alone or in combination (MTX, HCQ, SSZ or LEF)

Outcomes

- ACR20/ACR50/ACR70

- DAS28

- Total sharp score

- HAQ-DI score

- SF-36 PCS and MCS

- EQ-5D (VAS and utility scores)

- AEs leading to drop-outs

- Randomized controlled trials

Other

- Studies published in English

- Primary study available as full text published manuscript only; no study available as a conference abstract only was included with the exception of abstracts pertaining to investigational products, baricitinib and sarilumab

G.2 Criteria for studies to be selected from the systematic literature review and included in the NMA

The following criteria were used to select relevant studies to be included in the NMA:

Population

- Adult (>18 years) patients with moderate to severe RA who have had inadequate response to cDMARDs and are bDMARD-naive

Interventions

- Biologics as monotherapy or in combination with cDMARDs (adalimumab, certolizumab pegol, etanercept, golimumab, infliximab, abatacept, rituximab, tocilizumab, sarilumab, tofacitinib, baricitinib)

Comparators

- cDMARDs

- Any active comparator that allows for an indirect comparison between the bDMARDs of interest

Outcomes

- ACR20/ACR50/ACR70 at 6 months follow-up

G.3 Identified evidence base

Figure 11 summarizes the study identification and selection process. Of the 181 studies included in the large systematic literature review, 79 studies concerned the bDMARD-naive population (table NMA studies). There were 66 studies evaluating 36 interventions for which ACR response criteria were reported at 6 months (with a tolerability window of ± 4 weeks). The corresponding evidence network is presented in Figure 12. For the network meta-analysis the following were deemed to be clinically equivalent and were pooled.

- "INF 3mg/kg q8w" or "INF 5mg/kg q8w" or "INF 6mg/kg q8w"

- "ETN 50mg qw" or "ETN 25mg biw"

- "ABA 10mg/kg q4wa or"ABA SC 125mg qw"

- "CER 200mg q2w+MTX" or "CER 400mg q4w+MTX

- DMARDs including methotrexate, sulfasalazine, hydroxychloroquine, leflunomide at any dosage; studies which only described DMARD therapy as conventional or nonbiologic

G.4 Statistical models for network-meta analysis

G.4.1 ACR 20/50/70 response

The probability of ACR20/50/70 responses was estimated using a Bayesian (random effects) network meta-analyses model for ordered categorical data (Dias et al. 2013). The model assumes that there is an underlying continuous variable (ACR20/50/70) categorized by specifying different cutoffs corresponding to the point at which an individual moves from one category to the next in each trial. The advantage of this approach over an analysis that considers ACR categories separately is that all possible outcomes are analyzed simultaneously based on the same randomized controlled trials, allowing for consistent estimates by category. To avoid influencing the observed results by prior belief, uninformative prior distributions were used for the estimated model parameters. The relative treatment effects for each bDMARD versus cDMARDs estimated on the probit scale were
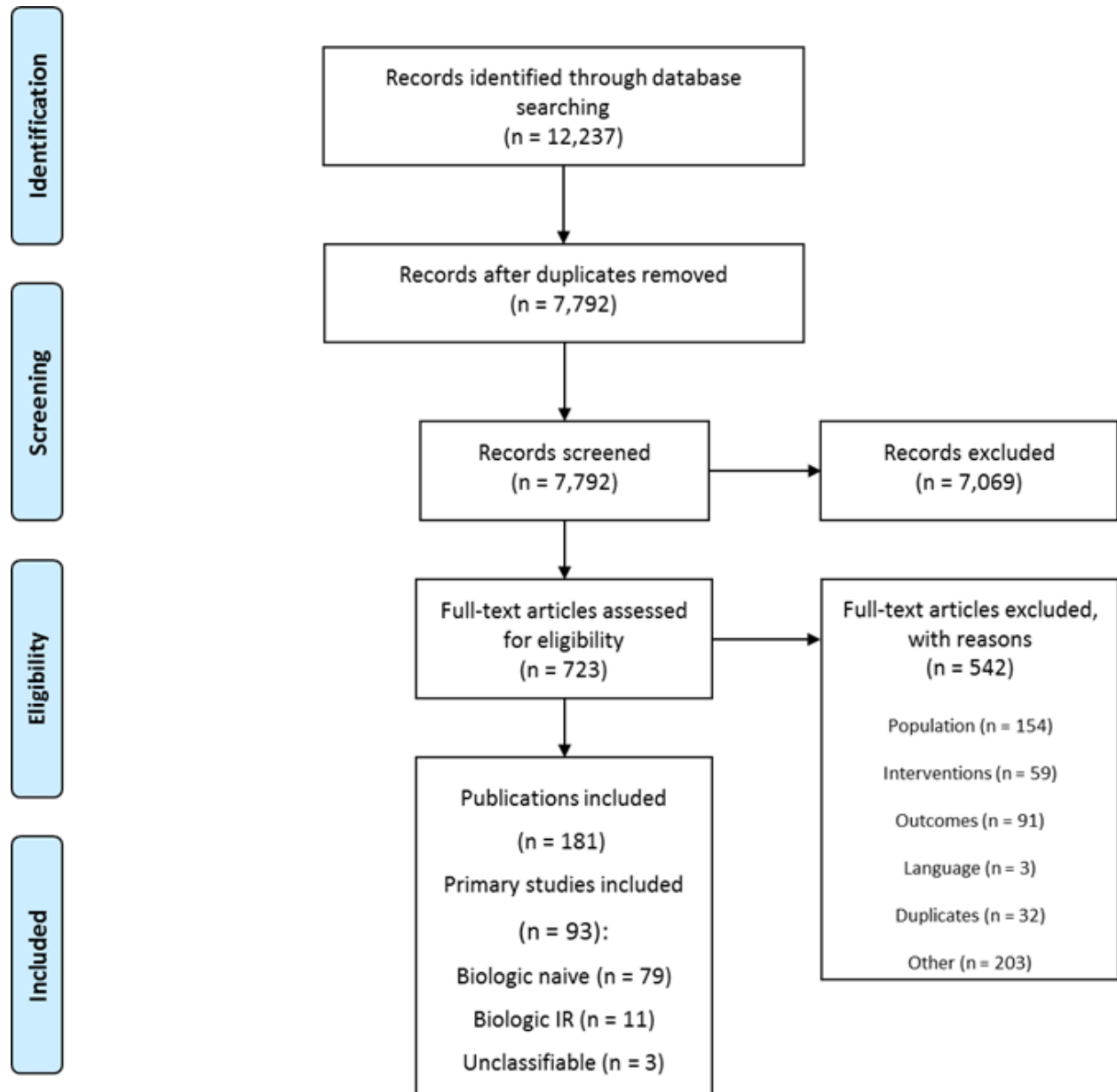
Figure 11: Study identification and selection

Figure 12: Bayesian random effects NMA network diagram for patients naive to bD-MARDs

transformed into absolute probabilities of the nonoverlapping ACR response categories by combining them with the average results for cDMARDs. The posterior distributions of parameters of interest were summarized by the median as a reflection of the point estimate and 95% credible intervals, constructed from the 2.5 and 97.5 percentiles. Analyses were performed with the Markov chain Monte Carlo method using the JAGS software package (http://mcmc-jags.sourceforge.net/).

Table 25: A comparison of NICE and IVI estimates of ACR response probabilities

	IVI			NICE		
	ACR20	ACR50	ACR70	ACR20	ACR50	ACR70
cdmards	0.26 (0.23-0.30)	0.10 (0.08-0.12)	0.03 (0.02-0.04)	0.298	0.123	0.042
abtivmtx	0.56 (0.47-0.65)	0.31 (0.23-0.40)	0.14 (0.09-0.20)	0.573	0.328	0.156
adamtx	0.56 (0.47-0.65)	0.31 (0.24-0.40)	0.14 (0.10-0.20)	0.615	0.368	0.183
etnmtx	0.64 (0.52-0.77)	0.40 (0.27-0.53)	0.20 (0.12-0.31)	0.713	0.472	0.263
golmtx	0.59 (0.45-0.74)	0.35 (0.22-0.50)	0.17 (0.09-0.28)	0.642	0.395	0.202
ifxmtx	0.66 (0.42-0.88)	0.43 (0.20-0.69)	0.23 (0.07-0.48)	0.595	0.348	0.169
tczmtx	0.56 (0.36-0.74)	0.32 (0.16-0.48)	0.15 (0.06-0.27)	0.706	0.464	0.256
czpmtx	0.31 (0.11-0.57)	0.14 (0.03-0.33)	0.05 (0.01-0.15)	0.564	0.319	0.150
abtscmtx	0.56 (0.41-0.70)	0.32 (0.19-0.45)	0.15 (0.07-0.24)	0.638	0.391	0.199
rtxmtx	0.57 (0.41-0.72)	0.33 (0.19-0.47)	0.15 (0.07-0.26)	0.573	0.328	0.156
tofmtx	0.60 (0.42-0.77)	0.35 (0.20-0.53)	0.17 (0.08-0.30)	-	-	-

Notes: ACR20/50/70 categories are the probability of at least a 20/50/70% improvement. 95% credible intervals are in parentheses. IVI estimates are based on 6-month simulations of 1,000 patients and 1,000 parameters sets for each therapy. NICE estimates are from Table 37 in Stevenson et al. (2017). cDMARDs = conventional disease-modifying antirheumatic drugs; MTX = methotrexate; ABT IV = abatacept intravenous; ADA = adalimumab; ETN = etanercept; GOL = golimumab; IFX = infliximab; TCZ = tocilizumab; CZP = certolizumab pegol; ABT SC = abatacept subcutaneous; RTX = rituximab; TOF = tofacitinib. ACR = American College of Rheumatology.

G.4.2 HAQ

G.4.3 DAS28

References

Alava, M. H., Wailoo, A., Wolfe, F., and Michaud, K. (2013). The relationship between eq-5d, haq and pain in patients with rheumatoid arthritis. *Rheumatology*, 52(5):944–950.

Alava, M. H., Wailoo, A. J., and Ara, R. (2012). Tails from the peak district: adjusted limited dependent variable mixture models of eq-5d questionnaire health state utility values. *Value in Health*, 15(3):550–561.

Aletaha, D., Nell, V. P., Stamm, T., Uffmann, M., Pflugbeil, S., Machold, K., and Smolen, J. S. (2005). Acute phase reactants add little to composite disease activity indices for rheumatoid arthritis: validation of a clinical activity score. *Arthritis research & therapy*, 7(4):R796.

Aletaha, D. and Smolen, J. (2005). The simplified disease activity index (sdai) and the clinical disease activity index (cdai): a review of their usefulness and validity in rheumatoid arthritis. *Clinical and experimental rheumatology*, 23(5):S100.

Anderson, J., Caplan, L., Yazdany, J., Robbins, M. L., Neogi, T., Michaud, K., Saag, K. G., O'dell, J. R., and Kazi, S. (2012). Rheumatoid arthritis disease activity measures: American college of rheumatology recommendations for use in clinical practice. *Arthritis care & research*, 64(5):640–647.

Arias, E. (2015). United states life tables, 2011. *National vital statistics reports: from the Centers for Disease Control and Prevention, National Center for Health Statistics, National Vital Statistics System*, 64(11):1–62.

Baio, G. and Dawid, A. P. (2015). Probabilistic sensitivity analysis in health economics. *Statistical methods in medical research*, 24(6):615–634.

Bojke, L., Claxton, K., Sculpher, M., and Palmer, S. (2009). Characterizing structural uncertainty in decision analytic models: a review and application of methods. *Value in Health*, 12(5):739–749.

Carlson, J. J., Ogale, S., Dejonckheere, F., and Sullivan, S. D. (2015). Economic evaluation of tocilizumab monotherapy compared to adalimumab monotherapy in the treatment of severe active rheumatoid arthritis. *Value in Health*, 18(2):173–179.

Claxton, K., Sculpher, M., McCabe, C., Briggs, A., Akehurst, R., Buxton, M., Brazier, J., and O'Hagan, T. (2005). Probabilistic sensitivity analysis for nice technology assessment: not an optional extra. *Health economics*, 14(4):339–347.

Claxton, L., Jenks, M., Taylor, M., Wallenstein, G., Mendelsohn, A. M., Bourret, J. A., Singh, A., Moynagh, D., and Gerber, R. A. (2016). An economic evaluation of tofacitinib treatment in rheumatoid arthritis: Modeling the cost of treatment strategies in the united states. *Journal of managed care & specialty pharmacy*, 22(9):1088–1102.

Curtis, J. R., Jain, A., Askling, J., Bridges, S. L., Carmona, L., Dixon, W., Finckh, A., Hyrich, K., Greenberg, J. D., Kremer, J., et al. (2010). A comparison of patient characteristics and outcomes in selected european and us rheumatoid arthritis registries. In *Seminars in arthritis and rheumatism*, volume 40, pages 2–14. Elsevier.

Deighton, C., Hyrich, K., Ding, T., Ledingham, J., Lunt, M., Luqmani, R., Kiely, P., Bukhari, M., Abernethy, R., Ostor, A., et al. (2010). Bsr and bhpr rheumatoid arthritis guidelines on eligibility criteria for the first biological therapy. *Rheumatology*, 49(6):1197–1199.

Dias, S., Sutton, A. J., Ades, A., and Welton, N. J. (2013). Evidence synthesis for decision making 2: a generalized linear modeling framework for pairwise and network meta-analysis of randomized controlled trials. *Medical Decision Making*, 33(5):607–617.

Gibson, L., Alava, M. H., and Wailoo, A. (2015). Progression of disease in people with rheumatoid arthritis treated with non biologic therapies. Technical report.

Gomez-Reino, J. J. and Carmona, L. (2006). Switching tnf antagonists in patients with chronic arthritis: an observational study of 488 patients over a four-year period. *Arthritis research & therapy*, 8(1):R29.

Guyot, P., Ades, A., Ouwens, M. J., and Welton, N. J. (2012). Enhanced secondary analysis of survival data: reconstructing the data from published kaplan-meier survival curves. *BMC medical research methodology*, 12(1):9.

Heath, A., Manolopoulou, I., and Baio, G. (2016). Estimating the expected value of partial perfect information in health economic evaluations using integrated nested laplace approximation. *Statistics in medicine*, 35(23):4264–4280.

Hernández Alava, M., Wailoo, A., Wolfe, F., and Michaud, K. (2014). A comparison of direct and indirect methods for the estimation of health utilities from clinical outcomes. *Medical Decision Making*, 34(7):919–930.

Institute for Clinical and Economic Review (2017). Targeted immune modulators for rheumatoid arthritis: Effectiveness & value. Technical report.

Jalal, H., Dowd, B., Sainfort, F., and Kuntz, K. M. (2013). Linear regression metamodeling as a tool to summarize and present simulation model results. *Medical Decision Making*, 33(7):880–890.

Jalal, H., Goldhaber-Fiebert, J. D., and Kuntz, K. M. (2015). Computing expected value of partial sample information from probabilistic sensitivity analysis using linear regression metamodeling. *Medical Decision Making*, 35(5):584–595.

Madan, J., Ades, T., Barton, P., Bojke, L., Choy, E., Helliwell, P., Jobanputra, P., Stein, K., Stevens, A., Tosh, J., et al. (2015). Consensus decision models for biologics in rheumatoid and psoriatic arthritis: recommendations of a multidisciplinary working party. *Rheumatology and Therapy*, 2(2):113–125.

Michaud, K., Vera-Llonch, M., and Oster, G. (2012). Mortality risk by functional status and health-related quality of life in patients with rheumatoid arthritis. *The Journal of rheumatology*, 39(1):54–59.

Michaud, K., Wallenstein, G., and Wolfe, F. (2011). Treatment and nontreatment predictors of health assessment questionnaire disability progression in rheumatoid arthritis: a longitudinal study of 18,485 patients. *Arthritis care & research*, 63(3):366–372.

Norton, S., Fu, B., Scott, D. L., Deighton, C., Symmons, D. P., Wailoo, A. J., Tosh, J., Lunt, M., Davies, R., Young, A., et al. (2014). Health assessment questionnaire disability progression in early rheumatoid arthritis: systematic review and analysis of two inception cohorts. In *Seminars in arthritis and rheumatism*, volume 44, pages 131–144. Elsevier.

Norton, S., Sacker, A., Dixey, J., Done, J., Williams, P., and Young, A. (2013). Trajectories of functional limitation in early rheumatoid arthritis and their association with mortality. *Rheumatology*, page ket253.

Oppong, R., Kaambwa, B., Nuttall, J., Hood, K., Smith, R. D., and Coast, J. (2013). The impact of using different tariffs to value eq-5d health state descriptions: an example from a study of acute cough/lower respiratory tract infections in seven countries. *The European journal of health economics*, 14(2):197–209.

Pan, S. M. D., Dehler, S., Ciurea, A., Ziswiler, H.-R., Gabay, C., and Finckh, A. (2009). Comparison of drug retention rates and causes of drug discontinuation between anti–tumor necrosis factor agents in rheumatoid arthritis. *Arthritis Care & Research*, 61(5):560–568.

Prevoo, M., Van't Hof, M., Kuper, H., Van Leeuwen, M., Van De Putte, L., and Van Riel, P. (1995). Modified disease activity scores that include twenty-eight-joint counts development and validation in a prospective longitudinal study of patients with rheumatoid arthritis. *Arthritis & Rheumatology*, 38(1):44–48.

Ramiro, S., Sepriano, A., Chatzidionysiou, K., Nam, J. L., Smolen, J. S., van der Heijde, D., Dougados, M., van Vollenhoven, R., Bijlsma, J. W., Burmester, G. R., et al. (2017). Safety of synthetic and biological dmards: a systematic literature review informing the 2016 update of the eular recommendations for management of rheumatoid arthritis. *Annals of the rheumatic diseases*, pages annrheumdis–2016.

Sarzi-Puttini, P., Fiorini, T., Panni, B., Turiel, M., Cazzola, M., and Atzeni, F. (2002). Correlation of the score for subjective pain with physical disability, clinical and radiographic scores in recent onset rheumatoid arthritis. *BMC musculoskeletal disorders*, 3(1):18.

Singh, J. A., Saag, K. G., Bridges, S. L., Akl, E. A., Bannuru, R. R., Sullivan, M. C., Vaysbrot, E., McNaughton, C., Osani, M., Shmerling, R. H., et al. (2016). 2015 american college of rheumatology guideline for the treatment of rheumatoid arthritis. *Arthritis & rheumatology*, 68(1):1–26.

Singh, J. A., Wells, G. A., Christensen, R., Tanjong Ghogomu, E., Maxwell, L. J., MacDonald, J. K., Filippini, G., Skoetz, N., Francis, D. K., Lopes, L. C., et al. (2011). Adverse effects of biologics: a network meta-analysis and cochrane overview. *The Cochrane Library*.

Smolen, J., Breedveld, F., Schiff, M., Kalden, J., Emery, P., Eberl, G., Van Riel, P., and Tugwell, P. (2003). A simplified disease activity index for rheumatoid arthritis for use in clinical practice. *Rheumatology*, 42(2):244–257.

Souto, A., Maneiro, J. R., and Gómez-Reino, J. J. (2015). Rate of discontinuation and drug survival of biologic therapies in rheumatoid arthritis: a systematic review and meta-analysis of drug registries and health care databases. *Rheumatology*, 55(3):523–534.

Stephens, S., Botteman, M. F., Cifaldi, M. A., and van Hout, B. A. (2015). Modelling the cost-effectiveness of combination therapy for early, rapidly progressing rheumatoid arthritis by simulating the reversible and irreversible effects of the disease. *BMJ open*, 5(6):e006560.

Stevenson, M., Archer, R., Tosh, J., Simpson, E., Everson-Hock, E., Stevens, J., Hernandez-Alava, M., Paisley, S., Dickinson, K., Scott, D., et al. (2016). Adalimumab, etanercept, infliximab, certolizumab pegol, golimumab, tocilizumab and abatacept for the treatment of rheumatoid arthritis not previously treated with disease-modifying antirheumatic drugs and after the failure of conventional disease-modifying antirheumatic drugs only: systematic review and economic evaluation. *Health Technology Assessment*, 20(35):1–610.

Stevenson, M. D., Wailoo, A. J., Tosh, J. C., Hernandez-Alava, M., Gibson, L. A., Stevens, J. W., Archer, R. J., Simpson, E. L., Hock, E. S., Young, A., et al. (2017). The cost-effectiveness of sequences of biological disease-modifying antirheumatic drug treatment in england for patients with rheumatoid arthritis who can tolerate methotrexate. *The Journal of Rheumatology*, pages jrheum–160941.

Strand, V., Williams, S., Miller, P., Saunders, K., Grant, S., and Kremer, J. (2013). Op0064 discontinuation of biologic therapy in rheumatoid arthritis (ra): Analysis from the consortium of rheumatology researchers of north america (corrona) database. *Annals of the Rheumatic Diseases*, 72(Suppl 3):A71–A72.

Tosh, J., Brennan, A., Wailoo, A., and Bansback, N. (2011). The sheffield rheumatoid arthritis health economic model. *Rheumatology*, 50(suppl 4):iv26–iv31.

Wailoo, A., Brennan, A., Bansback, N., Nixon, R., Wolfe, F., and Michaud, K. (2006). Modeling the cost effectiveness of etanercept, adalimumab and anakinra compared to infliximab in the treatment of patients with rheumatoid arthritis in the medicare program. *Rockville, MD: Agency for Healthcare Research and Quality.*

Wailoo, A. J., Bansback, N., Brennan, A., Michaud, K., Nixon, R. M., and Wolfe, F. (2008). Biologic drugs for rheumatoid arthritis in the medicare program: a cost-effectiveness analysis. *Arthritis & Rheumatology*, 58(4):939–946.

Wolfe, F. and Michaud, K. (2010). The loss of health status in rheumatoid arthritis and the effect of biologic therapy: a longitudinal observational study. *Arthritis research & therapy*, 12(2):R35.

Wolfe, F., Michaud, K., Choi, H. K., and Williams, R. (2005). Household income and earnings losses among 6,396 persons with rheumatoid arthritis. *The Journal of rheumatology*, 32(10):1875–1883.

Wolfe, F., Michaud, K., Gefeller, O., and Choi, H. K. (2003). Predicting mortality in patients with rheumatoid arthritis. *Arthritis & Rheumatism*, 48(6):1530–1542.

Yazici, Y., Krasnokutsky, S., Barnes, J. P., Hines, P. L., Wang, J., and Rosenblatt, L. (2009). Changing patterns of tumor necrosis factor inhibitor use in 9074 patients with rheumatoid arthritis. *The Journal of rheumatology*, 36(5):907–913.

Zhang, J., Shan, Y., Reed, G., Kremer, J., Greenberg, J. D., Baumgartner, S., and Curtis, J. R. (2011). Thresholds in disease activity for switching biologics in rheumatoid arthritis patients: experience from a large us cohort. *Arthritis care & research*, 63(12):1672–1679.